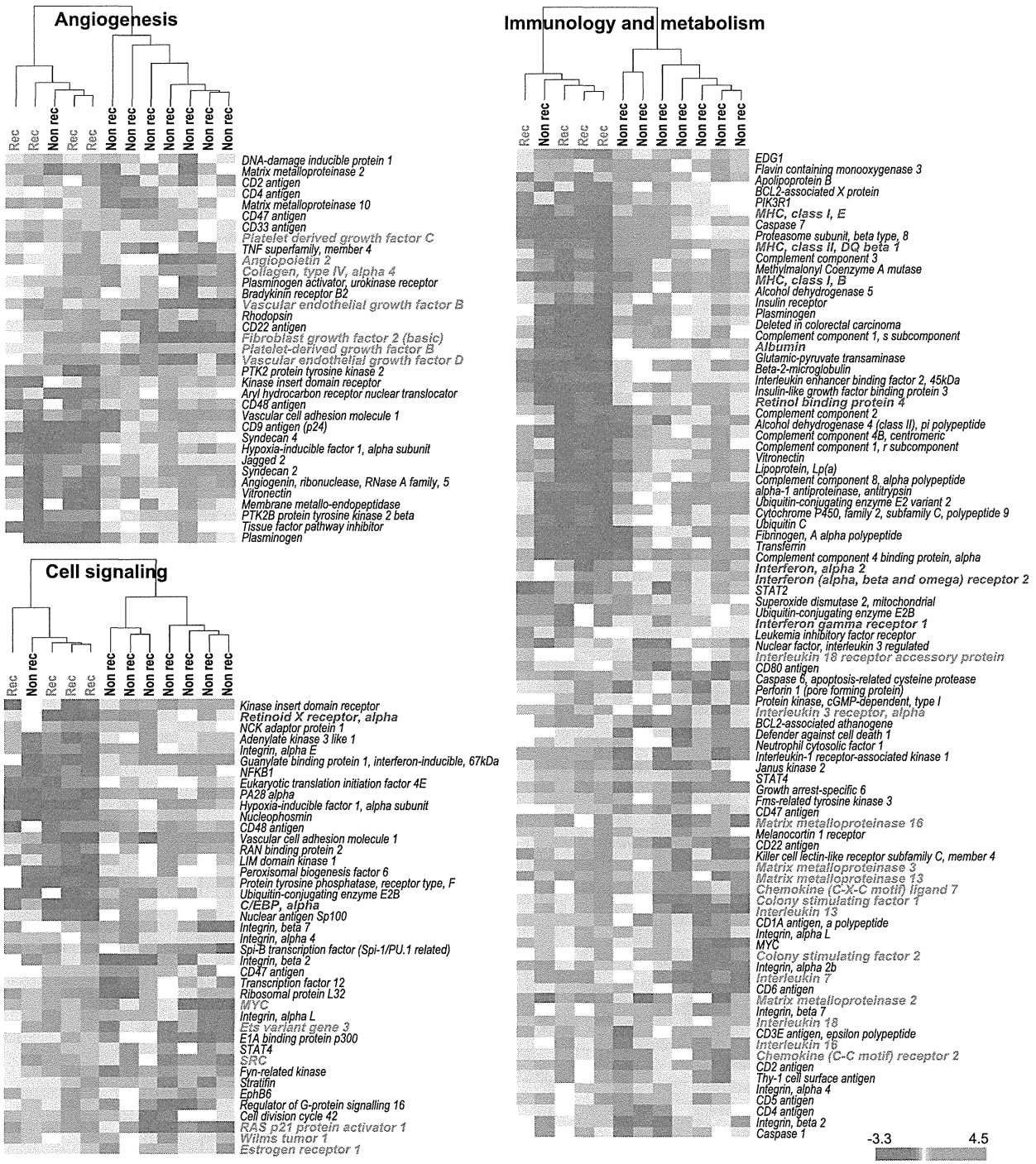

Figure 3 Hierarchical clustering using pre-defined curated gene sets based on NCBI's Cancer Genome Anatomy Project. Presented genes were differentially expressed at *P*-values <0.05 between patients with and without HCC recurrence.

of hepatic gene expression without peretinoin administration. Therefore, there might be some limitations in drawing concrete conclusions from this study.

Although we attempted to analyze the liver peretinoin concentration in the present study to investigate its possible relationship with gene expression, peretinoin levels were too low to yield a meaningful result. However, considering that gene expression profiling identified significant changes in the expression levels of retinoid-related and other genes before and during peretinoin treatment, we believe that sufficient levels of peretinoin reached the liver.

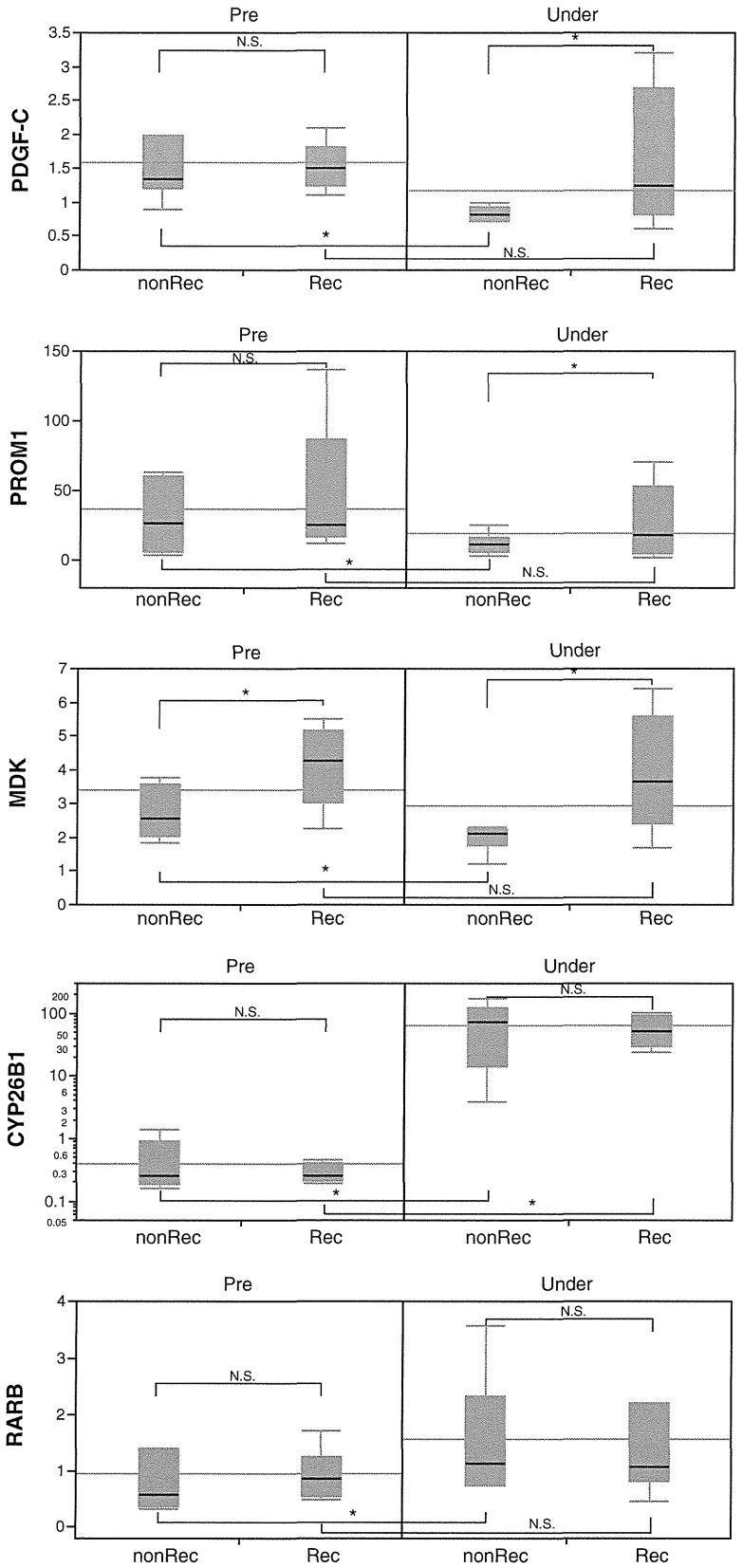

Figure 4 RTD-PCR evaluation of PDGF-C, PROM1, MDK, CYP26B1, and RAR β in the liver of patients with or without HCC recurrence.

The previous peretinoin phase II/III clinical study demonstrated that daily doses of 600 mg peretinoin significantly reduced the incidence of HCC recurrence in HCV-positive patients who underwent definitive treatment. The findings of the present study are complementary to this as we successfully identified candidates for the peretinoin-responsive and recurrence-related genes. These genes are probably involved in the inhibition of HCC recurrence and could be beneficial as future candidate biomarkers of the effectiveness of peretinoin.

Conclusions

In this study, patients underwent liver biopsy before and after 8 weeks of treatment with repeated doses of peretinoin. Gene expression profiling at week 8 of peretinoin treatment could successfully predict HCC recurrence within 2 years. This study is the first to show the effect of peretinoin in suppressing HCC recurrence *in vivo* based on gene expression profiles and provides a molecular basis for understanding the efficacy of peretinoin.

Additional files

Additional file 1: Study protocol.

Additional file 2: Figure S1. One-way hierarchical clustering of up-regulated or down-regulated genes in the liver by the administration of peretinoin (300 mg and 600 mg). Changes in gene expression in the liver before the start of peretinoin administration and 8 weeks into the treatment are shown. Patients with HCC recurrence within 2 years are shown in red and those with HCC recurrence after the cessation of peretinoin are boxed in red.

Additional file 3: Figure S2. Schematic representation of peretinoin action in the liver.

Abbreviations

ACR: Acyclic Retinoid; CH-C: Chronic Hepatitis C; HCC: Hepatocellular Carcinoma; HCV: Hepatitis C Virus.

Competing interests

The authors declare that they have no competing interests.

Authors' contributions

MH: study concept and design, manuscript preparation. TY: gene expression analysis. TY: acquisition of data of clinical data. KA: acquisition of data of clinical data. YS: gene expression analysis. AS: acquisition of data of clinical data. MN: gene expression analysis. EM: acquisition of data of clinical. SK: study concept and design. All authors read and approved the final manuscript.

Acknowledgements

The authors thank Nami Nishiyama for excellent technical assistance. This work was supported in part by KOWA Co. Ltd., Tokyo, Japan.

Received: 13 September 2012 Accepted: 8 March 2013
Published: 15 April 2013

References

1. Ferlay J, Shin HR, Bray F, Forman D, Mathers C, Parkin DM: **Estimates of worldwide burden of cancer in 2008: GLOBOCAN 2008.** *Int J Cancer* 2010, **127**(12):2893–2917.
2. Altekruse SF, McGlynn KA, Reichman ME: **Hepatocellular carcinoma incidence, mortality, and survival trends in the United States from 1975 to 2005.** *J Clin Oncol* 2009, **27**(9):1485–1491.
3. Llovet JM, Burroughs A, Bruix J: **Hepatocellular carcinoma.** *Lancet* 2003, **362**(9399):1907–1917.
4. Llovet JM, Bru C, Bruix J: **Prognosis of hepatocellular carcinoma: the BCLC staging classification.** *Semin Liver Dis* 1999, **19**(3):329–338.
5. Mazzaferro V, Regalia E, Doci R, Andreola S, Pulvirenti A, Bozzetti F, Montalto F, Ammatuna M, Morabito A, Gennari L: **Liver transplantation for the treatment of small hepatocellular carcinomas in patients with cirrhosis.** *N Engl J Med* 1996, **334**(11):693–699.
6. Llovet JM, Schwartz M, Mazzaferro V: **Resection and liver transplantation for hepatocellular carcinoma.** *Semin Liver Dis* 2005, **25**(2):181–200.
7. Castells A, Bruix J, Bru C, Fuster J, Vilana R, Navasa M, Ayuso C, Boix L, Visa J, Rodes J: **Treatment of small hepatocellular carcinoma in cirrhotic patients: a cohort study comparing surgical resection and percutaneous ethanol injection.** *Hepatology* 1993, **18**(5):1121–1126.
8. Shiratori Y, Shiina S, Teratani T, Imamura M, Obi S, Sato S, Koike Y, Yoshida H, Omata M: **Interferon therapy after tumor ablation improves prognosis in patients with hepatocellular carcinoma associated with hepatitis C virus.** *Ann Intern Med* 2003, **138**(4):299–306.
9. Breitenstein S, Dimitroulis D, Petrowsky H, Puhan MA, Mullhaupt B, Clavien PA: **Systematic review and meta-analysis of interferon after curative treatment of hepatocellular carcinoma in patients with viral hepatitis.** *Br J Surg* 2009, **96**(9):975–981.
10. Samuel M, Chow PK, Chan Shih-Yen E, Machin D, Soo KC: **Neoadjuvant and adjuvant therapy for surgical resection of hepatocellular carcinoma.** *Cochrane Database Syst Rev* 2009, **1**:CD001199.
11. Mathurin P, Raynard B, Dharancy S, Kirzin S, Fallik D, Pruvot FR, Roumilhac D, Canva V, Paris JC, Chaput JC, *et al*: **Meta-analysis: evaluation of adjuvant therapy after curative liver resection for hepatocellular carcinoma.** *Aliment Pharmacol Ther* 2003, **17**(10):1247–1261.
12. Muto Y, Moriwaki H, Ninomiya M, Adachi S, Saito A, Takasaki KT, Tanaka T, Tsurumi K, Okuno M, Tomita E, *et al*: **Prevention of second primary tumors by an acyclic retinoid, polyprenoic acid, in patients with hepatocellular carcinoma. Hepatoma Prevention Study Group.** *N Engl J Med* 1996, **334**(24):1561–1567.
13. Muto Y, Moriwaki H, Saito A: **Prevention of second primary tumors by an acyclic retinoid in patients with hepatocellular carcinoma.** *N Engl J Med* 1999, **340**(13):1046–1047.
14. Sano T, Kagawa M, Okuno M, Ishibashi N, Hashimoto M, Yamamoto M, Suzuki R, Kohno H, Matsushima-Nishiwaki R, Takano Y, *et al*: **Prevention of rat hepatocarcinogenesis by acyclic retinoid is accompanied by reduction in emergence of both TGF-alpha-expressing oval-like cells and activated hepatic stellate cells.** *Nutr Cancer* 2005, **51**(2):197–206.
15. Kagawa M, Sano T, Ishibashi N, Hashimoto M, Okuno M, Moriwaki H, Suzuki R, Kohno H, Tanaka T: **An acyclic retinoid, NIK-333, inhibits N-diethylnitrosamin-einduced rat hepatocarcinogenesis through suppression of TGF-alpha expression and cell proliferation.** *Carcinogenesis* 2004, **25**(6):979–985.
16. Okusaka T, Ueno H, Ikeda M, Morizane C: **Phase I and pharmacokinetic clinical trial of oral administration of the acyclic retinoid NIK-333.** *Hepatol Res* 2011, **41**(6):542–552.
17. Okita K, Matsui O, Kumada H, Tanaka K, Kaneko S, Moriwaki H, Izumi N, Okusaka T, Ohashi Y, Makuuchi M: **Effect of peretinoin on recurrence of hepatocellular carcinoma (HCC): Results of a phase II/III randomized placebo-controlled trial.** *J Clin Oncol* 2010, **15s**(28Suppl):4024.
18. Honda M, Yamashita T, Ueda T, Takatori H, Nishino R, Kaneko S: **Different signaling pathways in the livers of patients with chronic hepatitis B or chronic hepatitis C.** *Hepatology* 2006, **44**(5):1122–1138.
19. Honda M, Sakai A, Yamashita T, Nakamoto Y, Mizukoshi E, Sakai Y, Yamashita T, Nakamura M, Shirasaki T, Horimoto K, *et al*: **Hepatic ISG expression is associated with genetic variation in interleukin 28B and the outcome of IFN therapy for chronic hepatitis C.** *Gastroenterology* 2010, **139**(2):499–509.
20. Nakamura N, Shidoji Y, Yamada Y, Hatakeyama H, Moriwaki H, Muto Y: **Induction of apoptosis by acyclic retinoid in the human hepatoma-derived cell line, HuH-7.** *Biochem Biophys Res Commun* 1995, **207**(1):382–388.
21. Yasuda I, Shiratori Y, Adachi S, Obora A, Takemura M, Okuno M, Shidoji Y, Seishima M, Muto Y, Moriwaki H: **Acyclic retinoid induces partial differentiation, down-regulates telomerase reverse transcriptase mRNA**

expression and telomerase activity, and induces apoptosis in human hepatoma-derived cell lines. *J Hepatol* 2002, **36**(5):660–671.
22. Yamada Y, Shidoji Y, Fukutomi Y, Ishikawa T, Kaneko T, Nakagama H, Imawari M, Moriwaki H, Muto Y: **Positive and negative regulations of albumin gene expression by retinoids in human hepatoma cell lines.** *Mol Carcinog* 1994, **10**(3):151–158.
23. Suzui M, Masuda M, Lim JT, Albanese C, Pestell RG, Weinstein IB: **Growth inhibition of human hepatoma cells by acyclic retinoid is associated with induction of p21(CIP1) and inhibition of expression of cyclin D1.** *Cancer Res* 2002, **62**(14):3997–4006.
24. Suzui M, Shimizu M, Masuda M, Lim JT, Yoshimi N, Weinstein IB: **Acyclic retinoid activates retinoic acid receptor beta and induces transcriptional activation of p21(CIP1) in HepG2 human hepatoma cells.** *Mol Cancer Ther* 2004, **3**(3):309–316.
25. Muto Y, Moriwaki H: **Antitumor activity of vitamin A and its derivatives.** *J Natl Cancer Inst* 1984, **73**(6):1389–1393.
26. Sakabe T, Tsuchiya H, Endo M, Tomita A, Ishii K, Gonda K, Murai R, Takubo K, Hoshikawa Y, Kurimasa A, *et al*: **An antioxidant effect by acyclic retinoid suppresses liver tumor in mice.** *Biochem Pharmacol* 2007, **73**(9):1405–1411.
27. Okada H, Honda M, Campbell JS, Sakai Y, Yamashita T, Takebuchi Y, Hada K, Shirasaki T, Takabatake R, Nakamura M, *et al*: **Acyclic retinoid targets platelet-derived growth factor signaling in the prevention of hepatic fibrosis and hepatocellular carcinoma development.** *Cancer Res* 2012, **72**(17):4459–4471.
28. Tomaru Y, Nakanishi M, Miura H, Kimura Y, Ohkawa H, Ohta Y, Hayashizaki Y, Suzuki M: **Identification of an inter-transcription factor regulatory network in human hepatoma cells by Matrix RNAi.** *Nucleic Acids Res* 2009, **37**(4):1049–1060.
29. Nakanishi M, Tomaru Y, Miura H, Hayashizaki Y, Suzuki M: **Identification of transcriptional regulatory cascades in retinoic acid-induced growth arrest of HepG2 cells.** *Nucleic Acids Res* 2008, **36**(10):3443–3454.
30. Uray IP, Shen Q, Seo HS, Kim H, Lamph WW, Bissonnette RP, Brown PH: **Rexinoid-induced expression of IGFBP-6 requires RARbeta-dependent permissive cooperation of retinoid receptors and AP-1.** *J Biol Chem* 2009, **284**(1):345–353.
31. Ma Y, Koza-Taylor PH, DiMattia DA, Hames L, Fu H, Dragnev KH, Turi T, Beebe JS, Freemantle SJ, Dmitrovsky E: **Microarray analysis uncovers retinoid targets in human bronchial epithelial cells.** *Oncogene* 2003, **22**(31):4924–4932.
32. Ye X, Tao Q, Wang Y, Cheng Y, Lotan R: **Mechanisms underlying the induction of the putative human tumor suppressor GPRC5A by retinoic acid.** *Cancer Biol Ther* 2009, **8**(10):951–962.
33. Llovet JM, Bruix J: **Molecular targeted therapies in hepatocellular carcinoma.** *Hepatology* 2008, **48**(4):1312–1327.
34. Zender L, Villanueva A, Tovar V, Sia D, Chiang DY, Llovet JM: **Cancer gene discovery in hepatocellular carcinoma.** *J Hepatol* 2010, **52**(6):921–929.
35. Datta J, Majumder S, Kutay H, Motiwala T, Frankel W, Costa R, Cha HC, MacDougald OA, Jacob ST, Ghoshal K: **Metallothionein expression is suppressed in primary human hepatocellular carcinomas and is mediated through inactivation of CCAAT/enhancer binding protein alpha by phosphatidylinositol 3-kinase signaling cascade.** *Cancer Res* 2007, **67**(6):2736–2746.
36. Fields AL, Soprano DR, Soprano KJ: **Retinoids in biological control and cancer.** *J Cell Biochem* 2007, **102**(4):886–898.
37. Hoshida Y, Villanueva A, Kobayashi M, Peix J, Chiang DY, Camargo A, Gupta S, Moore J, Wrobel MJ, Lerner J, *et al*: **Gene expression in fixed tissues and outcome in hepatocellular carcinoma.** *N Engl J Med* 2008, **359**(19):1995–2004.
38. Utsunomiya T, Shimada M, Imura S, Morine Y, Ikemoto T, Mori M: **Molecular signatures of noncancerous liver tissue can predict the risk for late recurrence of hepatocellular carcinoma.** *J Gastroenterol* 2010, **45**(2):146–152.

doi:10.1186/1471-2407-13-191
Cite this article as: Honda *et al.*: Peretinoin, an acyclic retinoid, improves the hepatic gene signature of chronic hepatitis C following curative therapy of hepatocellular carcinoma. *BMC Cancer* 2013 **13**:191.

THE JOURNAL OF BIOLOGICAL CHEMISTRY VOL. 289, NO. 1, pp. 335–345, January 3, 2014

Metformin Suppresses Expression of the Selenoprotein P Gene via an AMP-activated Kinase (AMPK)/FoxO3a Pathway in H4IIEC3 Hepatocytes*[S]

Received for publication, May 1, 2013, and in revised form, November 18, 2013 Published, JBC Papers in Press, November 20, 2013, DOI 10.1074/jbc.M113.479386

Hiroaki Takayama,[a] Hirofumi Misu,[a] Hisakazu Iwama,[b] Keita Chikamoto,[a,c] Yoshiro Saito,[d] Koji Murao,[e] Atsushi Teraguchi,[f] Fei Lan,[a] Akihiro Kikuchi,[a] Reina Saito,[a] Natsumi Tajima,[a] Takayoshi Shirasaki,[a,g] Seiichi Matsugo,[h,i] Ken-ichi Miyamoto,[j,k] Shuichi Kaneko,[a] and Toshinari Takamura[a1]

From the [a]Department of Disease Control and Homeostasis, Kanazawa University Graduate School of Medical Sciences, 13-1 Takara-machi, Kanazawa, Ishikawa 920-8641, Japan, the [b]Life Science Research Center, Kagawa University, Ikenobe 1750-1, Miki-cho, Kita-gun, Kagawa 761-0793, Japan, the [c]Division of Natural System, Graduate School of Natural Science and Technology, Kanazawa University, Kakuma-machi, Kanazawa, Ishikawa 920-1192, Japan, the [d]Systems Life Sciences, Department of Medical Life Systems, Faculty of Medical and Life Sciences, Doshisha University, Kyotanabe, Kyoto 610-0394, Japan, the [e]Departments of Advanced Medicine, Kagawa University, Ikenobe 1750-1, Miki-cho, Kita-gun, Kagawa 761-0793, Japan, the [f]Department of Hospital Pharmacy, Kanazawa University, 13-1 Takara-machi, Kanazawa, Ishikawa 920-8641, Japan, the [g]Department of Advanced Medical Technology, Kanazawa University Graduate School of Health Medicine, 13-1 Takara-machi, Kanazawa, Ishikawa 920-8641, Japan, the [h]Division of Material Engineering, Graduate School of Natural Science and Technology, Kanazawa University, Kakuma-machi, Kanazawa, Ishikawa 920-1192, Japan, the [i]Institute of Science and Engineering, Faculty of Natural System, Kanazawa University, Kakuma-machi, Kanazawa, Ishikawa 920-1192, Japan, the [j]Department of Hospital Pharmacy, Kanazawa University Graduate School of Medical Sciences, 13-1 Takara-machi, Kanazawa, Ishikawa 920-8641, Japan, and the [k]Department of Medicinal Informatics, Kanazawa University Graduate School of Medical Sciences, 13-1 Takara-machi, Kanazawa, Ishikawa 920-8641, Japan

Background: The suppression of selenoprotein P production may be a novel therapeutic target for reducing insulin resistance.
Results: Selenoprotein P expression was suppressed by metformin treatment, but co-administration of AMPK inhibitor or FoxO3a siRNA cancelled this suppression.
Conclusion: Metformin suppresses selenoprotein P expression via the AMPK/FoxO3a pathway.
Significance: The AMPK/FoxO3a pathway in the liver may be a therapeutic target for type 2 diabetes.

Selenoprotein P (SeP; encoded by *SEPP1* in humans) is a liver-derived secretory protein that induces insulin resistance in type 2 diabetes. Suppression of SeP might provide a novel therapeutic approach to treating type 2 diabetes, but few drugs that inhibit *SEPP1* expression in hepatocytes have been identified to date. The present findings demonstrate that metformin suppresses *SEPP1* expression by activating AMP-activated kinase (AMPK) and subsequently inactivating FoxO3a in H4IIEC3 hepatocytes. Treatment with metformin reduced *SEPP1* promoter activity in a concentration- and time-dependent manner; this effect was cancelled by co-administration of an AMPK inhibitor. Metformin also suppressed *Sepp1* gene expression in the liver of mice. Computational analysis of transcription factor binding sites conserved among the species resulted in identification of the FoxO-binding site in the metformin-response element of the *SEPP1* promoter. A luciferase reporter assay showed that metformin suppresses Forkhead-response element activity, and a ChIP assay revealed that metformin decreases binding of FoxO3a, a direct target of AMPK, to the *SEPP1* promoter. Transfection with siRNAs for *Foxo3a*, but not for *Foxo1*, cancelled metformin-induced luciferase activity suppression of the metformin-response element of the *SEPP1* promoter. The overexpression of FoxO3a stimulated *SEPP1* promoter activity and rescued the suppressive effect of metformin. Metformin did not affect FoxO3a expression, but it increased its phosphorylation and decreased its nuclear localization. These data provide a novel mechanism of action for metformin involving improvement of systemic insulin sensitivity through the regulation of SeP production and suggest an additional approach to the development of anti-diabetic drugs.

Selenoprotein P (SeP[2]; encoded by *SEPP1* in humans) is a secretory protein produced mainly by the liver (1, 2). SeP contains 10 selenocysteine residues and is known to transport the essential trace element selenium from the liver to the rest of the

* This work was supported by grants-in-aid from the Ministry of Education, Culture, Sports, Science and Technology, Japan (to H. M., T. T., and S. K.) and research grants from Dainippon Sumitomo Pharma (to S. K.) and Takeda Science Foundation (to H. M.).
[S] This article contains supplemental Figs. S1–S5.
[1] To whom correspondence should be addressed: Dept. of Disease Control and Homeostasis, Kanazawa University Graduate School of Medical Science, 13-1 Takara-machi, Kanazawa, Ishikawa 920-8641, Japan. Tel.: 81-76-265-2233; Fax: 81-76-234-4250; E-mail: ttakamura@m-kanazawa.jp.

[2] The abbreviations used are: SeP, selenoprotein P; AMPK, AMP-activated kinase; AICAR, 5-aminoimidazole-4-carboxamide ribonucleotide; compound C, 6-[4-(2-piperidin-1-yl-ethoxy)-phenyl)]-3-pyridin-4-yl-pyrrazolo[1,5-a]-pyrimidine; cGPx, cellular glutathione peroxidase; DN, dominant negative; CA, constitutive active; TFBS, transcription factor binding site; FHRE, forkhead-response element.

body (3, 4). Our laboratory reported recently that SeP functions as a hepatokine that contributes to insulin resistance in type 2 diabetes (5). Using comprehensive gene expression analyses in humans, hepatic gene expression levels of *SEPP1* were found to be positively correlated with the severity of insulin resistance in patients with type 2 diabetes. Moreover, treatment with purified SeP protein impairs insulin signal transduction in both cell culture and animal models. Importantly, the RNA interference-mediated knockdown of SeP improves insulin resistance and hyperglycemia in a mouse model of type 2 diabetes, suggesting that the suppression of SeP production in the liver may be a novel therapeutic target for reducing insulin resistance in type 2 diabetes (5). However, few drugs that inhibit the production of SeP by hepatocytes have been identified to date.

Metformin is widely used as an anti-diabetic drug globally. The primary target of metformin action is the liver, which abundantly expresses organic cation transporter (Oct)-1, a transporter for metformin (6, 7). Adenosine monophosphate-activated protein kinase (AMPK) mediates primarily the glucose-lowering actions of metformin, including the suppression of hepatic gluconeogenesis (8). In contrast, several reports indicate that the oral administration of metformin in humans increases insulin sensitivity in skeletal muscle, increases serum adiponectin, and improves aortic arteriosclerosis (9–11). These reports suggest that orally administered metformin also exerts beneficial actions on tissues other than the liver, in which expression levels of Octs are lower. To date, however, the molecular mechanisms underlying the systemic actions of metformin are not fully understood.

Forkhead box protein O3a (FoxO3a), which belongs to the Forkhead transcription factors of the FoxO subfamily (FoxOs), is reported to be involved in cell cycle arrest (12), apoptosis (13), and the oxidative stress response (14, 15). Recently, Greer *et al.* (16) showed that FoxO3a, but not FoxO1, is directly phosphorylated and activated by AMPK *in vitro*. FoxO3a is reported to positively regulate mitochondria-related genes, such as uncoupling proteins, in mouse embryonic fibroblasts, suggesting that the direct regulation of FoxO3a by AMPK plays a crucial role in the control of the cellular energy balance. The phosphorylation of FoxO3a by AMPK was also identified in C2C12 myotubes (17), aortic vascular endothelial cells (18), and A549 lung cancer cells (19). However, the role of the AMPK/FoxO3a pathway in hepatocytes, an important target of metformin, remains unknown.

We demonstrate here that metformin suppresses *SEPP1* gene expression by activating AMPK and subsequently inactivating FoxO3a in H4IIEC3 hepatocytes. These results suggest a novel mechanism underlying the glucose-lowering action of metformin.

EXPERIMENTAL PROCEDURES

Materials—The antibodies against AMPKα, phospho-AMPKα, FoxO1, FoxO3a, acetylated Lys, and Lamin A/C were purchased from Cell Signaling Technology (Beverly, MA). Antibody against phospho-Ser/Thr/Tyr was purchased from AnaSpec (San Jose, CA). Antibody against GAPDH was purchased from Santa Cruz Biotechnology, Inc. 5-Aminoimidazole-4-carboxamide ribonucleotide (AICAR) and 6-[4-(2-Piperidin-1-yl-ethoxy)-phenyl)]-3-pyridin-4-yl-pyrrazolo [1,5-a]-pyrimidine (compound C) were purchased from Sigma-Aldrich. FoxO3a expression vector was provided from Ajinomoto Pharma (Tokyo, Japan) described before (20). Selenious acid was purchased from WaKo Pure Chemical Industries, Ltd. (Osaka, Japan). Metformin was provided by Dainippon Sumitomo Pharma (Osaka, Japan).

Generation of Plasmid Constructs—The human *SEPP1* promoter region has been described previously (21). Fragments of ~1800 bp from the human *SEPP1* promoter region and the deletion promoter region were amplified by PCR using normal human genomic DNA as a template and the primer pairs shown in Table 1. The PCR product was subcloned into the luciferase reporter gene plasmid pGL3-basic (Promega, Madison, WI) and termed "*SEPP1*-Promoter-Luc," "Mut-A," "Mut-B," "Mut-C," "Mut-D," "Mut-E," "Mut-DΔ1," "Mut-DΔ2," and "Mut-DΔ3." Putative FoxO binding site-deficient vector were generated using QuikChange Lightning site-directed mutagenesis kits (Agilent Technologies, Santa Clara, CA), according to the manufacturer's instructions. All inserts were confirmed by DNA sequencing.

Cell Culture—Studies were performed using the rat hepatoma cell line H4IIEC3 (American Type Culture Collection, Manassas, VA). Cells were cultured in Dulbecco's modified Eagle's medium (DMEM; Invitrogen) and supplemented with 10% fetal bovine serum (Invitrogen), 2 mmol/liter L-glutamine (WaKo Pure Chemical Industries, Ltd.), 100 units/ml penicillin, and 0.1 mg/ml streptomycin (WaKo Pure Chemical Industries, Ltd.). The cells were cultured at 37 °C in a humidified atmosphere containing 5% CO_2.

Measurement of Glutathione Peroxidase Activity—To measure cellular glutathione peroxidase (cGPx) activity, a coupled enzyme assay, which was performed by following the oxidation of NADPH, was used as described previously (22). In brief, cells were cultured with 1) DMEM plus 10% FBS, 2) DMEM plus 10% FBS and 100 nM selenious acid, or 3) DMEM plus 10% FBS and 1000 nM selenious acid at 72 h. Then cells were fractured with homogenate buffer containing 0.25 M sucrose, 50 mM Tris-HCl (pH 7.4), 0.1 mM EDTA, 0.1 mM 2-mercaptoethanol. The assay conditions were as follows for the cGPx assay: 0.1 M phosphate buffer, pH 7.4, 0.2 mM NADPH, 0.5 mM EDTA, 1 mM NaN_3, 2 mM GSH, 1 unit/ml GSH reductase, and 30 μM hydrogen peroxide. The oxidation of NADPH was followed at 340 nm at 37 °C, and units of the enzyme activity were expressed as μmol of NADPH oxidized/min.

Transfection and Luciferase Reporter Gene Assay—H4IIEC3 cells were grown in 24-well plates and transfected with 0.4 μg of plasmid DNA/well together with 1.2 μl of FuGENE6 (Promega). For the luciferase reporter gene assays, 0.4 μg of firefly luciferase promoter construct was co-transfected with 0.01 μg of *Renilla* luciferase control plasmid (pRL-SV40; Promega) and/or 0.05–0.4 μg of plasmids expressing FoxO3a or empty control plasmids, resulting in a total DNA amount of 0.41–0.81 μg/well. 24 h later, cells were treated with the indicated reagents, such as metformin, in DMEM plus 10% FBS for the indicated times. After 48 h, luciferase activities were measured using the Dual Luciferase assay system (Promega), as described previously (20).

TABLE 1
Primers used in cloning

Primer	Description	Sequence
***SEPP1*-Promoter-Luc**		
Forward	hSeP-promoter-F-BglII	ACTAGATCTACAAACCTTTCAGACACTGAGTTG
Reverse	hSeP-promoter-R-NcoI	ACTCCATGGACAACCACTTCCAACGGGCCTGCTT
Mut-A		
Forward	hSeP-promoter-Del-F1-BglII	ACTAGATCTGGGCTGCCTGTCTTTGATTTCACAT
Reverse	hSeP-promoter-R-NcoI	ACTCCATGGACAACCACTTCCAACGGGCCTGCTT
Mut-B		
Forward	hSeP-promoter-Del-F2-BglII	ACTAGATCTTTGTAGTTCCTGCACCTTGTACAAC
Reverse	hSeP-promoter-R-NcoI	ACTCCATGGACAACCACTTCCAACGGGCCTGCTT
Mut-C		
Forward	hSeP-promoter-Del-F3-BglII	ACTAGATCTGCATAGGTCTTCCAGGAAGTACGAC
Reverse	hSeP-promoter-R-NcoI	ACTCCATGGACAACCACTTCCAACGGGCCTGCTT
Mut-D		
Forward	hSeP-promoter-Del-F4-BglII	ACTAGATCTCAAATGTTTTTCCCTGTTATAGTTT
Reverse	hSeP-promoter-R-NcoI	ACTCCATGGACAACCACTTCCAACGGGCCTGCTT
Mut-E		
Forward	hSeP-promoter-F-BglII	ACTAGATCTACAAACCTTTCAGACACTGAGTTG
Reverse	hSeP-promoter-Del-R1-NocI	ACTCCATGGCTGAGCCAGCGAATTATGCTGCTGC
Mut-DΔ1		
Forward	hSeP-promoter-Del-F14-BglII	ACTAGATCTGATTCTAGGGTGACTGAAAAGGATA
Reverse	hSeP-promoter-R-NcoI	ACTCCATGGACAACCACTTCCAACGGGCCTGCTT
Mut-DΔ2		
Forward	hSeP-promoter-Del-F15-BglII	ACTAGATCTATAACAATCAGCTCAGGGGTTTGCT
Reverse	hSeP-promoter-R-NcoI	ACTCCATGGACAACCACTTCCAACGGGCCTGCTT
Mut-DΔ3		
Forward	hSeP-promoter-Del-F16-BglII	ACTAGATCTATAAATATCAGAGTGTGCTGCTGTG
Reverse	hSeP-promoter-R-NcoI	ACTCCATGGACAACCACTTCCAACGGGCCTGCTT
Mut-DΔ2-ΔFoxo A		
Forward	del86–95	GACTATACCTGAGGGGTGAGGGACTATAAATATCAGAGTG
Reverse	del86–95-antisense	CACTCTGATATTTATAGTCCCTCACCCCTCAGGTATAGTC
Mut-DΔ2-ΔFoxo B		
Forward	hSeP-del-Foxo 3-F	GAGGTAAACAACAGGACTAAGAGTGTGCTGCTGTGG
Reverse	hSeP-del-Foxo 3-R	CCACAGCAGCACACTCTTAGTCCTGTTGTTTACCTC

siRNA Transfection in H4IIEC3 Hepatocytes—H4IIEC3 hepatocytes were grown in 24-well plates and transiently transfected with 10 nM small interfering RNA (siRNA) duplex oligonucleotides using 1 μl of Lipofectamine™ RNAiMAX (Invitrogen) by the reverse transfection method according to the manufacturer's instructions. *Foxo1*- and *Foxo3a*-specific siRNAs with the following sequences were synthesized (Thermo Scientific): *Foxo1* A, 5′-GACAGCAAAUCAAGUUAUG-3′ (sense); *Foxo1* B, 5′-UUUGAUAACUGGAGUACAU-3′ (sense); *Foxo3a* A, 5′-GAACGUUGUUGGUUUGAAC-3′ (sense); and *Foxo3a* B, 5′-CGUCAUGGGUCACGACAAG-3′ (sense). Negative control siRNA was also utilized (Thermo Scientific). 24 h after transfection, the cells were treated with metformin for 24 h, followed by the extraction of total RNA.

Adenovirus-mediated Gene Transfer in H4IIEC3 Hepatocytes—Cells were transfected with adenoviruses as described previously (5). Briefly, H4IIEC3 hepatocytes were grown to 90% confluence in 24-well multiplates and transfected with adenoviruses encoding dominant negative (DN) α1 and α2 AMPK, constitutive active (CA) AMPK, or LacZ for 4 h. The cells were incubated with DMEM for 24 h after removing the adenoviruses; total RNA was then extracted.

Quantitative RT-PCR—Total RNA was extracted from cultured H4IIEC3 hepatocytes using a Genelute mammalian total RNA miniprep kit (Sigma). The reverse transcription of 100 ng of total RNA was performed using a high capacity cDNA reverse transcription kit (Invitrogen), according to the manufacturer's instructions. Quantitative RT-PCR was performed using TaqMan probes (ACTB, 4352340E; Foxo1, Rn01494868_m1; Foxo3, Rn01441087_m1; G6pc, Rn00565347_m1; Pck1, Rn01529014_m1; Sepp1, Rn00569905_m1) and the 7900HT fast real-time PCR system (Invitrogen), as described previously (23).

Western Blotting—Treated cells were collected and lysed as described previously (20). Protein samples (10 μg/lane) were subjected to SDS-PAGE and transferred to PVDF membranes using the iBlot Gel Transfer system (Invitrogen). The membranes were blocked, incubated with primary antibody, washed, and incubated with the secondary HRP-labeled antibody. Bands were visualized with the ECL Prime Western blotting Detection System (GE Healthcare) and LAS-3000 (Fujifilm, Tokyo, Japan). A densitometric analysis of blotted membranes was performed using ImageJ software.

Immunoprecipitation—Immunoprecipitation of serine/threonine/tyrosine-phosphorylated proteins or lysine-acetylated proteins was carried out using the Dynabeads protein G immunoprecipitation kit (Invitrogen) according to the manufacturer's instructions. The nuclear and cytoplasmic fractions were extracted using an NE-PER nuclear and cytoplasmic extraction reagent kit (Pierce).

Detection of the Conserved Transcription Factor Binding Sites Using Multiple-genome Alignments—The Ensembl 12-way Enredo-Pecan-Ortheus (EPO) eutherian multiple alignments (12-way EPO alignments) (24, 25) were downloaded. The 12-way EPO was excised to obtain the alignment block corresponding to the human genome coordinates from 10 kb upstream of the coding sequence of *SEPP1*, including the start

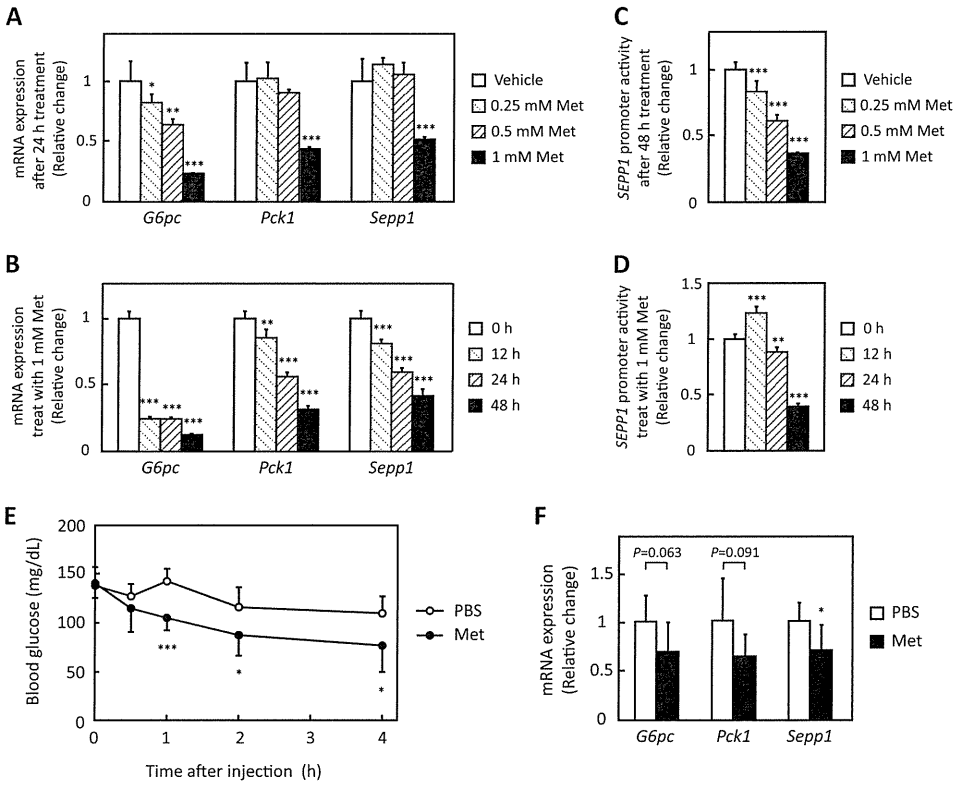

FIGURE 1. **Metformin suppressed *Sepp1* gene expression in H4IIEC3 hepatocytes and livers of C57BL/6J mice.** *A* and *B*, metformin suppressed *Sepp1* mRNA expression in a concentration- and time-dependent manner. H4IIEC3 cells were treated with the indicated concentrations of metformin for the indicated times. Expression values were normalized to *Actb* mRNA. Data represent means ± S.D. (*error bars*) ($n = 4$). *, $p < 0.05$; **, $p < 0.01$; ***, $p < 0.001$ *versus* vehicle-treated cells or 0 h. *C* and *D*, *SEPP1* promoter activity was suppressed in a concentration- and time-dependent manner. H4IIEC3 cells were co-transfected with the *SEPP1* promoter reporter vector and control reporter vector. 24 h later, the cells were treated with the indicated concentrations of metformin for the indicated times. Values were normalized to the activity of the control luciferase vector. Data represent means ± S.D. ($n = 4$). **, $p < 0.01$; ***, $p < 0.001$ *versus* vehicle-treated cells or 0 h. *E* and *F*, metformin suppressed *Sepp1* mRNA expression in livers of C57BL/6J mice. Following fasting for 4 h, 12-week-old female C57BL/6J mice were administrated 300 mg/kg metformin. 4 h after metformin administration, mice were sacrificed, and liver mRNA expression was examined. Expression values were normalized to *Actb* mRNA. Data represent means ± S.D. ($n = 7$). *, $p < 0.05$ *versus* PBS-injected mice.

codon. To predict the conserved transcription factor binding sites (TFBSs), the 10-kb upstream genome sequence for each of the 12 species was searched using the TRANSFAC (26) and the MATCH™ program (27) (version 6.1) with varied thresholds. Then the predicted TFBSs were mapped on the alignments, and the conserved TFBSs for *SEPP1* were identified.

Chromatin Immunoprecipitation (ChIP) Assay—A ChIP assay was carried out using the ChIP IT Express enzymatic kit (Active Motif, Carlsbad, CA) according to the manufacturer's instructions. In brief, HepG2 cells were treated with metformin 6 h before being fixed and homogenized. Following centrifugation, the supernatant was used for chromatin samples. Chromatin samples were incubated with protein G-coated magnetic beads and ChIP grade FoxO1 or FoxO3a antibodies (Abcam, Cambridge, MA) overnight at 4 °C. Following washing and elution, a reaction solution was used as the template for PCR. PCR primers were set for amplification of the Mut-DΔ2 region of the *SEPP1* promoter, as follows: forward, 5′-GCACTTGCTACTTTCTTTTAAGTTG-3′; reverse, 5′-CACAGCAGCACACTCTGATATTTAT-3′.

Animals—12-week-old C57BL/6J female mice were obtained from CLEA Japan, Inc. (Tokyo, Japan). All animals were housed in a 12-h light/dark cycle and allowed free access to food and water. Following the fasting for 4 h, mice were administrated 300 mg/kg metformin. 4 h later, mice were anesthetized and sacrificed to allow isolation of liver tissue.

Statistical Analysis—Results are expressed as means ± S.D. Significance was tested by one-way analysis of variance with the Bonferroni method, and differences were considered statistically significant at a p value of less than 0.05.

RESULTS

Metformin Suppresses SEPP1 Expression at the Promoter Level—The effects of metformin on *Sepp1* expression in H4IIEC3 hepatocytes were examined. Metformin suppressed *Sepp1* mRNA expression in a concentration- and time-dependent manner, similarly to *G6pc* and *Pck1*, which encode representative gluconeogenic enzymes glucose-6-phosphatase and phosphoenolpyruvate carboxykinase 1, respectively (Fig. 1, *A* and *B*). These results are consistent with a previous report using rat primary hepatocytes (28). Next, the effects of metformin on *SEPP1* promoter activity were examined. The human *SEPP1* promoter region was cloned to a luciferase reporter vector as reported previously (21). The present sequence completely corresponded to the reference sequence of the National Center for Biotechnology Information, but it missed one thymidine against the sequence of the previous report (accession number Y12262) (supplemental Fig. S1). Similar to the mRNA results,

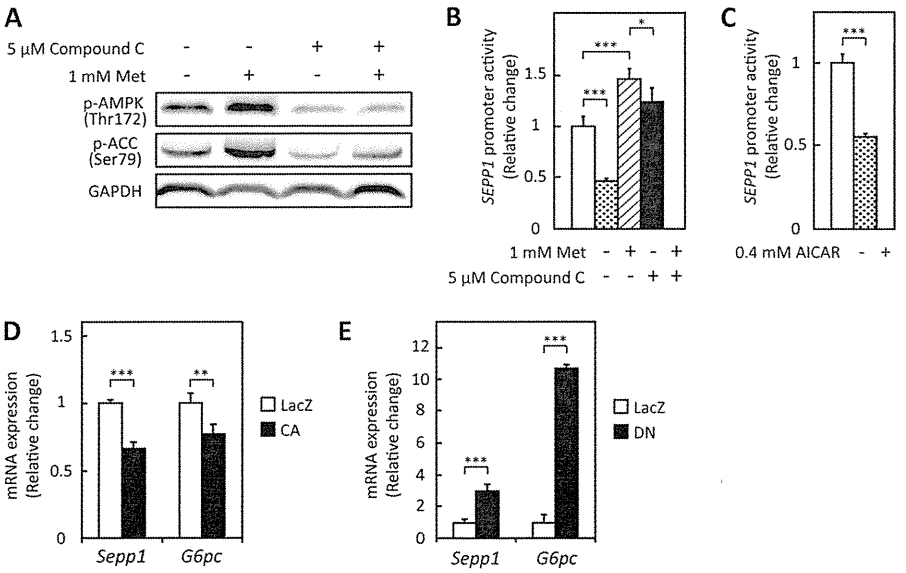

FIGURE 2. **Metformin suppressed *SEPP1* promoter activity via AMPK pathway in H4IIEC3 hepatocytes.** *A*, metformin-induced AMPK phosphorylation in the absence or presence of compound C. H4IIEC3 cells were treated with the indicated concentrations of metformin and compound C for 24 h. AMPK phosphorylation was examined by Western blotting. *B*, compound C treatment recovered metformin-induced suppression of the *SEPP1* promoter. H4IIEC3 cells were co-transfected with the *SEPP1* promoter reporter vector and control reporter vector at 24 h and then treated with the indicated concentrations of metformin and compound C for 48 h. Signals were normalized to the control reporter vector. Data represent means ± S.D. (*error bars*) ($n = 4$). ***, $p < 0.001$. *C*, AICAR suppressed *SEPP1* promoter activity. H4IIEC3 cells were co-transfected with the *SEPP1* promoter reporter vector and control reporter vector at 24 h and then treated with 0.4 mM AICAR for 24 h. Signals were normalized to the control reporter vector. Data represent means ± S.D. ($n = 4$). ***, $p < 0.001$. *D* and *E*, influence of adenoviruses carrying constitutive active (CA) or dominant negative (DN) AMPK. H4IIEC3 cells were infected with adenoviruses encoding CA-AMPK, DN-AMPK, or LacZ. Expression values were normalized to *Actb* mRNA. Data represent means ± S.D. ($n = 4$). **, $p < 0.01$; ***, $p < 0.001$.

metformin suppressed *SEPP1* promoter activity in a concentration- and time-dependent manner (Fig. 1, *C* and *D*), suggesting that it directly decreases *SEPP1* transcriptional activity in H4IIEC3 hepatocytes.

To confirm whether the present experimental condition (DMEM plus 10% FBS) supplied selenium sufficiently to synthesize selenoproteins for cultured cells, cGPx activity was measured with or without additional selenium supplement. Supplemental Fig. S2 indicates that supplementation of 100 or 1000 nM selenious acid to DMEM plus 10% FBS increased cGPx activity more than 3 times, suggesting that our experimental condition was insufficient to maximize selenoprotein synthesis. However, the current activity of cGPx in the cells cultured at DMEM plus 10% FBS (233 units/g) corresponded to the levels reported previously in the normal rat liver tissue (120–1800 units/g) (29, 30). Because these results suggest that the culture condition of DMEM plus 10% FBS was physiological, we used this condition in the following cellular experiments.

The action of metformin on *Sepp1* was also examined in mice. Following fasting for 4 h, 12-week-old female C57BL/6J mice were administrated 300 mg/kg metformin. Metformin decreased blood glucose levels by 30% (Fig. 1*E*) and tended to down-regulate gene expression for *G6pc* and *Pck1* after 4 h. Gene expression of *Sepp1* was significantly decreased by metformin (Fig. 1*F*). These results indicate that metformin suppresses gene expression for *Sepp1* in the liver of mice as well as in the cultured hepatocytes.

Metformin Suppresses SEPP1 Promoter Activity via AMPK Activation—Metformin is known to exert anti-diabetic effects by activating AMPK pathways (31). Hence, to determine whether AMPK pathways are involved in the metformin-induced suppression of *SEPP1* promoter activity, cells were treated with compound C, a representative AMPK inhibitor. Findings confirmed that the metformin-induced phosphorylation of AMPK and acetyl-CoA carboxylase was cancelled by the co-administration of compound C in H4IIEC3 hepatocytes (Fig. 2*A*). Co-administration of compound C partly rescued the cells from the inhibitory effects of metformin on the *SEPP1* promoter (Fig. 2*B*) and increased *SEPP1* promoter activity in the absence of metformin (Fig. 2*B*). In contrast, treatment with AICAR, a known activator of AMPK, decreased *SEPP1* promoter activity similarly to metformin (Fig. 2*C*). To determine whether AMPK pathways were involved in *SEPP1* promoter activity, H4IIEC3 hepatocytes were infected with an adenovirus encoding CA- or DN-AMPK. Transfection with CA-AMPK suppressed *Sepp1* and *G6pc* mRNA expression (Fig. 2*D*), whereas transfection with DN-AMPK enhanced *Sepp1* and *G6pc* mRNA expression (Fig. 2*E*). These results suggest that metformin decreases *SEPP1* promoter activity, at least partly, by activating AMPK.

Metformin-response Element in the SEPP1 Promoter Includes the FoxO Binding Site—To determine the nature of the metformin-response element in the *SEPP1* promoter region, several deletion mutants of the *SEPP1* promoter were constructed (Fig. 3*A*). Promoter activity of Mut-A to Mut-D, but not Mut-E, was suppressed by metformin treatment (Fig. 3*A*), indicating that the metformin-response element of the *SEPP1* promoter exists in Mut-D. Additional deletion mutants of Mut-D were constructed and named Mut-DΔ1 to DΔ3. Mut-DΔ1 and -DΔ2, but not Mut-DΔ3, were suppressed by metformin (Fig. 3*B*), indicating that the metformin-response element in the *SEPP1* promoter is localized in the Mut-DΔ2 sequence. Using computational analysis to identify conserved TFBSs among the species (see "Experimental Procedures"), several putative TFBSs were identified in the Mut-DΔ2 sequence (supplemental Fig. S3).

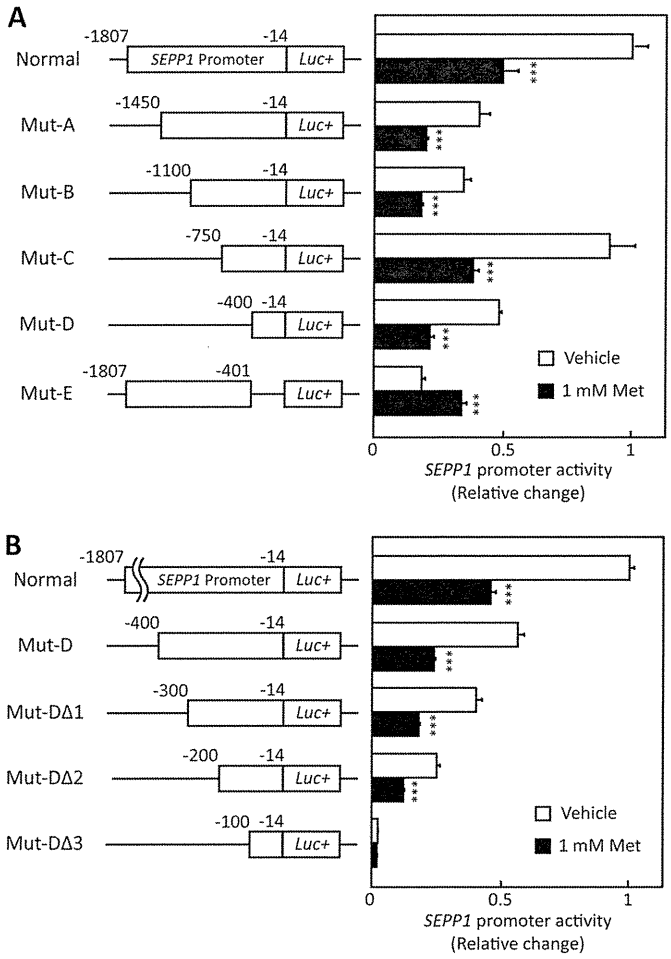

FIGURE 3. **SEPP1 promoter activity of deletion mutants.** *A* and *B*, structure and luciferase activity of promoter-deletion mutants. The sequences deleted within the constructs are shown as *thin lines*. The remaining parts of the *SEPP1* promoter were fused to a luciferase reporter gene. H4IIEC3 cells were co-transfected with each reporter vector and control reporter vector at 24 h and then treated with the indicated concentrations of metformin for 48 h. Signals were normalized to the control reporter vector. Data represent means ± S.D. (*error bars*) ($n = 4$). ***, $p < 0.001$ *versus* vehicle-treated cells.

Because early reports indicate that AMPK directly phosphorylates FoxO3a and regulates its transcriptional activity (16), this investigation focused on the two putative FoxO binding sites (Fig. 4*A*).

Metformin Suppresses FoxO Activity via AMPK Activation—To determine whether metformin treatment influences FoxO activity, a forkhead-response element (FHRE)-Luc vector that includes three tandems of FHREs ligated with a luciferase gene was utilized (32). This vector was used as a reporter of FoxO-responsive promoter activity (33). Metformin treatment suppressed FHRE activity, and concurrent treatment with compound C completely cancelled this suppression (Fig. 4*B*). In addition, treatment with compound C stimulated FHRE activity in the absence of metformin (Fig. 4*B*), whereas AICAR treatment suppressed FHRE activity (Fig. 4*C*). These results suggest that metformin suppresses FHRE activity via AMPK activation. To determine the critical FoxO binding site for metformin-induced *SEPP1* suppression, we constructed luciferase vectors that deleted either of two putative FoxO binding sites and were named Mut-DΔ2-ΔFoxo A or B, respectively (supplemental Fig. S4). Luciferase assay using these vectors revealed that putative FoxO binding site B was essential for metformin-induced *SEPP1* suppression (Fig. 4*D*). Because the assays using these vectors are not specific to FoxO3a activity, the interaction of FoxO proteins with DNA sequences in the *SEPP1* promoter was examined using a ChIP assay. For the ChIP assay, HepG2 cells were utilized to evaluate the human *SEPP1* promoter. Metformin suppressed *SEPP1* expression in HepG2 cells as well as H4IIEC3 cells (data not shown). The ChIP assay indicates that treatment with metformin decreased the binding of FoxO3a to *SEPP1* promoter, whereas it increased the binding of FoxO1 (Fig. 4*E*). These results suggest that FoxO3a, but not FoxO1, is associated with the metformin-induced suppression of *SEPP1* expression.

Metformin Suppresses SEPP1 Expression via FoxO3a Inactivation—Next, we examined whether the specific knockdown of endogenous *Foxo3a* or *Foxo1* affects *Sepp1* expression in H4IIEC3 hepatocytes. Transfection with *Foxo3a*- or *Foxo1*-specific siRNA resulted in a ~50% reduction in mRNA levels of *Foxo3a* or *Foxo1* (Fig. 5*A*). Knockdown of both *Foxo1* and *Foxo3a* resulted in a significant down-regulation of *Sepp1* expression (Fig. 5*A*). Interestingly, mRNA levels of *G6pc* were decreased by *Foxo3a* knockdown (Fig. 5*A*), suggesting that not only FoxO1 but also FoxO3a positively regulates the expression of the gluconeogenesis-related genes in H4IIEC3 hepatocytes. Next, we assessed whether knockdown of *Foxo3a* selectively affects the inhibitory action of metformin on the *SEPP1* promoter. Transfection with siRNAs for *Foxo3a*, but not for *Foxo1*, cancelled metformin-induced suppression of Mut-DΔ2 luciferase activity (Fig. 5*B*). These results suggest that the metformin-induced suppression of *Sepp1* is dependent on FoxO3a but not on FoxO1.

Whether FoxO3a overexpression influences the action of metformin on *SEPP1* promoter activity was also investigated. The FoxO3a protein was overexpressed in a concentration-dependent manner in cells transfected with the pCMV6-FoxO3a expression vector (Fig. 5*C*). Overexpression of FoxO3a significantly enhanced *SEPP1* promoter activity (Fig. 5*D*), and transfection with pCMV6-FoxO3a rescued the cells from the suppressive effect of metformin on *SEPP1* promoter activity in a concentration-dependent manner (Fig. 5, *D* and *E*). These results indicate that metformin decreases *SEPP1* promoter activity and gene expression via FoxO3a inactivation in H4IIEC3 hepatocytes.

Metformin Decreases FoxO3a Protein in the Nuclear Components—To elucidate the mechanism by which metformin inactivates FoxO3a, phosphorylation and acetylation of FoxO3a were examined in hepatocytes treated with metformin. Metformin treatment altered neither mRNA levels of *Foxo3a* (Fig. 6*A*) nor protein levels of FoxO3a (Fig. 6*B*). However, immunoprecipitation experiments revealed that treatment with metformin phosphorylated FoxO3a but not FoxO1 in H4IIEC hepatocytes (Fig. 6, *B* and *C*, and supplemental Fig. S5). Because a previous report indicated that FoxO3a, as well as FoxO1, is deacetylated by sirtuin family proteins downstream of AMPK (34), we examined the deacetylation of FoxO3a and FoxO1. Acetylation of both FoxO1 and FoxO3a was unaffected by metformin administration (Fig. 6, *B* and *C*, and supplemental Fig. S5). To determine the intracellular localization of FoxO3a, the cytosolic and

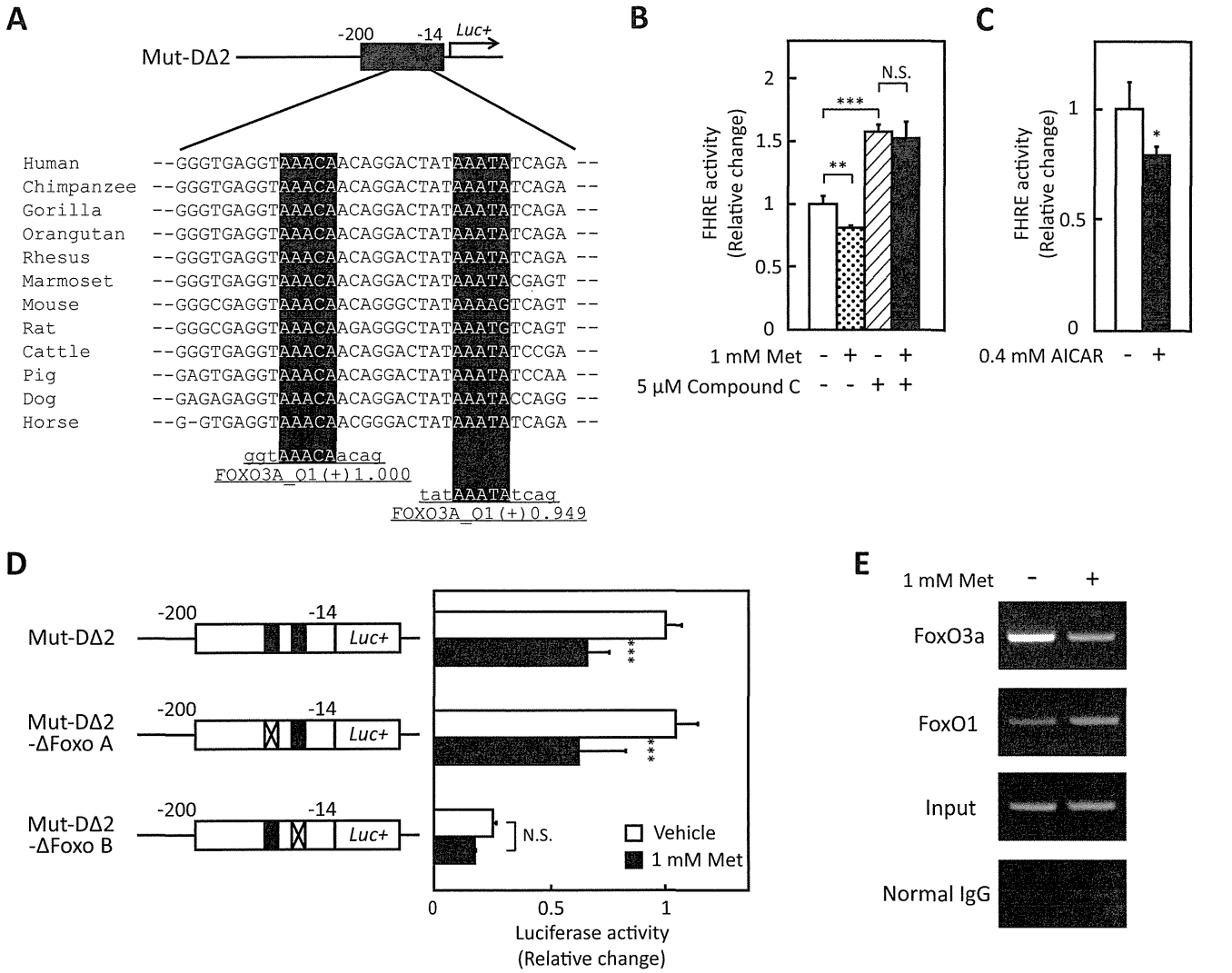

FIGURE 4. **Activation of the AMPK suppressed FoxO activity.** *A*, putative FoxO3a binding sites of Mut-DΔ2 sequence. Detection of the conserved TFBSs was performed using multiple-genome alignments and the *highlighted* putative transcriptional factor binding sites. *B*, FoxO activity in the absence or presence of metformin and compound C. H4IIEC3 cells were co-transfected with the FHRE-Luc vector and control reporter vector at 24 h and then treated with the indicated concentrations of metformin and compound C for 48 h. Signals were normalized to the control reporter vector. Data represent means ± S.D. (*error bars*) ($n = 4$). **, $p < 0.01$; ***, $p < 0.001$. *N.S.*, not significant. *C*, FoxO activity in the absence or presence of AICAR. H4IIEC3 cells were co-transfected with the FHRE-Luc vector and control reporter vector at 24 h and then treated with the indicated concentrations of AICAR for 24 h. Signals were normalized to the control reporter vector. Data represent means ± S.D. ($n = 4$). *, $p < 0.05$ *versus* vehicle-treated cells. *D*, deficiency of putative FoxO binding site cancelled metformin-induced suppression of *SEPP1* promoter activity. H4IIEC3 cells were co-transfected with each reporter vector and control reporter vector at 24 h and then treated with the indicated concentrations of metformin for 24 h. Signals were normalized to the control reporter vector. Data represent means ± S.D. ($n = 4$). ***, $p < 0.001$ *versus* vehicle-treated cells. *E*, chromatin immunoprecipitation assay of HepG2 cells treated with metformin. HepG2 cells were treated with metformin for 6 h. Chromatin samples precipitated with anti-FoxO3a, anti-FoxO1, or normal IgG were amplified using primers for the Mut-DΔ2 region of the human *SEPP1* promoter.

nuclear components of the FoxO3a protein were fractionated. FoxO3a and FoxO1 protein levels were decreased by metformin treatment in the nuclear fraction (Fig. 6*D*). These results suggest that metformin inactivates FoxO3a by decreasing FoxO3a protein levels in the nucleus and subsequently inhibiting the binding of FoxO3a to the *SEPP1* promoter.

DISCUSSION

Our data demonstrate that metformin suppresses production of the insulin resistance-inducing hepatokine SeP by activating AMPK and subsequently inactivating FoxO3a in H4IIEC3 hepatocytes. During the course of this study, it was reported that metformin decreases mRNA levels of *Sepp1* in rat primary hepatocytes (28); however, the molecular mechanisms by which metformin reduces the expression of *Sepp1* were not fully understood. Our data demonstrate that the AMPK/FoxO3a pathway downstream of metformin action plays a major role in the regulation of *SEPP1* expression in cultured hepatocytes. Our data suggest a previously unrecognized mechanism of action of metformin in combating the systemic insulin resistance in type 2 diabetes.

The finding that FoxO3a positively regulates *Sepp1* and *G6pc* expression in H4IIEC3 hepatocytes supports the suggestion that FoxO3a plays an important role in glucose homeostasis. The ability of FoxO1 to increase the expression of gluconeogenic genes has been confirmed (35). To date, however, little

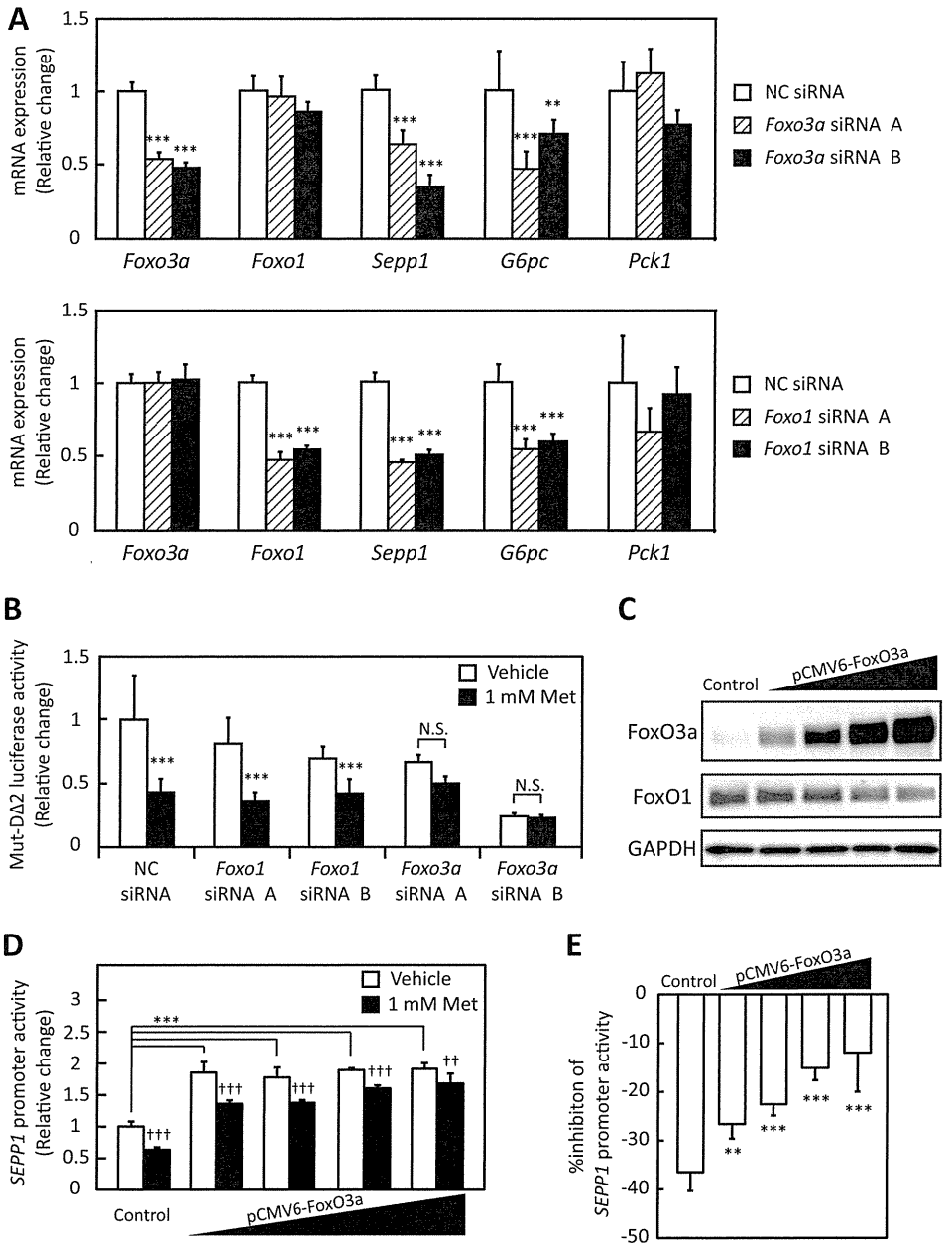

FIGURE 5. **Metformin suppressed SeP expression via FoxO3a.** *A*, efficiency of *Foxo3a* siRNA and *Foxo1* siRNA. H4IIEC3 cells were transfected with *Foxo3a* siRNAs or *Foxo1* siRNAs or a negative control (*NC*) siRNA at 48 h. Knockdown efficiency was assessed by real-time PCR. Expression values were normalized to *Actb* mRNA. Data represent means ± S.D. (*error bars*) ($n = 4$). **, $p < 0.01$; ***, $p < 0.001$ *versus* negative control siRNA-treated cells. *B*, luciferase activity of Mut-DΔ2 treated with *Foxo3a* or *Foxo1* siRNA and metformin. H4IIEC3 cells were transfected with *Foxo3a* siRNAs or *Foxo1* siRNAs or negative control siRNA at 24 h and then co-transfected with Mut-DΔ2 vector and control reporter vector. 24 h after transfection, cells were treated with the indicated concentrations of metformin for 24 h. Signals were normalized to the control reporter vector. Data represent means ± S.D. ($n = 4$). ***, $p < 0.001$ *versus* vehicle-treated cells. *N.S.*, not significant. *C*, protein levels in the presence of the FoxO3a overexpression vector. H4IIEC3 cells were transfected with the pCMV-FoxO3a vector or pCMV empty vector at 24 h. FoxO3a protein levels were then assessed by Western blotting. *D*, *SEPP1* promoter activity transfected with the FoxO3a overexpression vector. H4IIEC3 cells were co-transfected with the expression vectors for FoxO3a, *SEPP1* promoter reporter and control reporter at 24 h and then treated with the indicated concentrations of metformin for 48 h. Data represent means ± S.D. ($n = 3$–4). ***, $p < 0.001$ *versus* control; ††, $p < 0.01$; †††, $p < 0.001$ *versus* vehicle-treated cells. *E*, percentage inhibition of *SEPP1* promoter activity by metformin. Suppression ratios of *SEPP1* promoter activity were calculated based on the data in *E*. Data represent means ± S.D. ($n = 3$–4). **, $p < 0.01$; ***, $p < 0.001$ *versus* control.

information concerning the involvement of FoxO3a in glucose metabolism is available. Certainly, no defects in glucose metabolism have been described in FoxO3a-deficient mice (36), suggesting that the function of FoxO3a in glucose metabolism is compensated for by FoxO1. Indeed, Haeusler *et al.* (37) reported that triple liver-specific ablation of FoxO1, FoxO3a, and FoxO4 causes a more pronounced hypoglycemia and increased insulin sensitivity in mice compared with a single knockout of FoxO1. The present findings indicate that FoxO proteins, including FoxO3a, regulate hepatic glucose metabolism in a coordinated manner. These data reveal that FoxO3a, the downstream target of metformin/AMPK, positively regulates *SEPP1* transcriptional activity in cultured hepatocytes independently of FoxO1 and suggest that

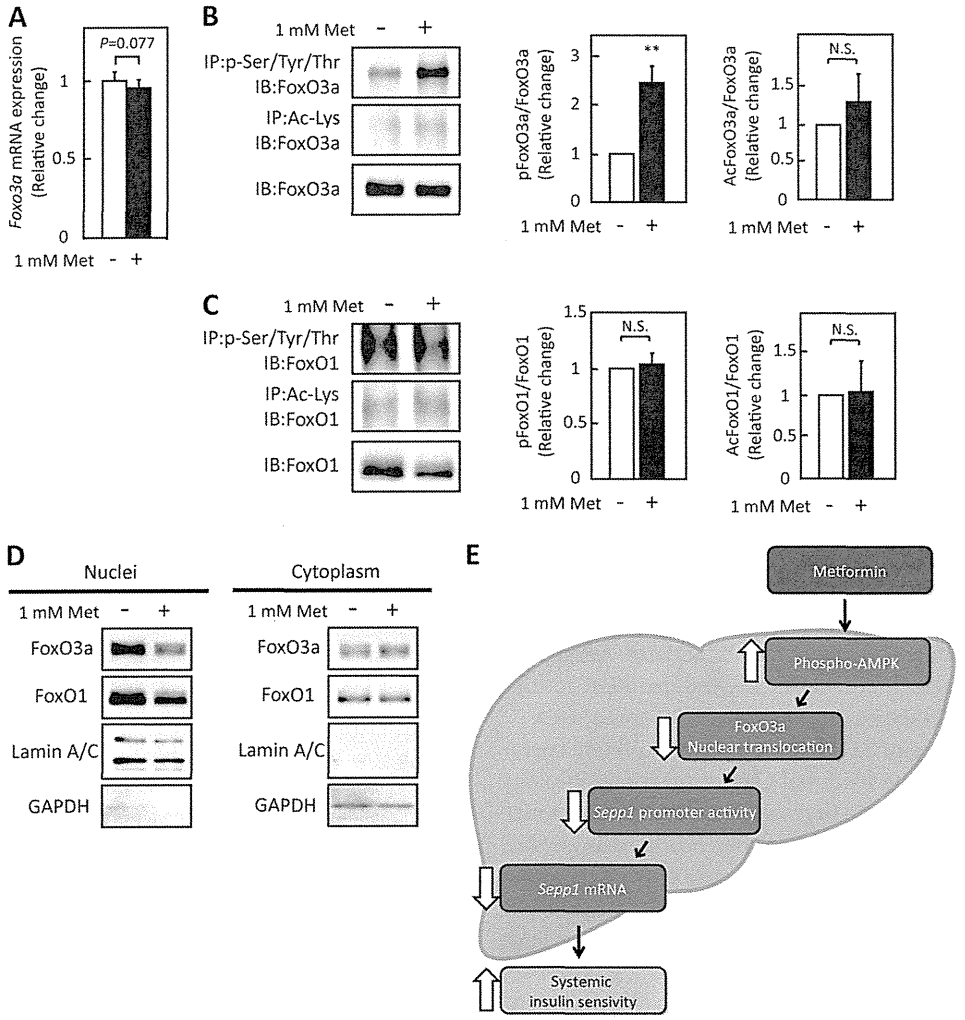

FIGURE 6. **Metformin treatment did not suppress FoxO3a expression but did suppress its activity.** *A*, *FoxO3a* mRNA expression in H4IIEC3 hepatocytes treated with metformin for 6 h. Expression values were normalized to *Actb* mRNA. Data represent means ± S.D. ($n = 5–6$). *B and C*, modification of FoxOs proteins by metformin treatment. Proteins were extracted after 6 h of metformin treatment. Immunoblotting was performed using anti-FoxO3a antibody (*B*) or anti-FoxO1 antibody (*C*). Data represent means ± S.D. ($n = 3$). **, $p < 0.01$. *N.S.*, not significant. *IP*, immunoprecipitation; *IB*, immunoblot. *D*, intracellular localization of FoxO3a and FoxO1 in H4IIEC3 hepatocytes upon treatment with metformin. Proteins were extracted after 6 h of metformin treatment. *E*, scheme of SeP suppression by metformin in the liver. FoxO3a positively regulates *SEPP1* promoter activity. Metformin suppresses FoxO3a activity via AMPK activation, resulting in suppression of SeP expression. Thus, the hypoglycemic effects of metformin may be mediated at least in part by SeP suppression in the liver.

FoxO3a participates in glucose homeostasis via regulation of the hepatic production of SeP, an insulin resistance-inducing hepatokine.

Knockdown of *Foxo3a*, but not *Foxo1*, rescued the cells from metformin-induced inactivation of the *SEPP1* promoter, although knockdown of both *Foxo3a* and *Foxo1* down-regulated *Sepp1* in the absence of metformin (Fig. 5, *A* and *B*). These results are in harmony with early reports showing that FoxO1 positively regulates *Sepp1* expression in cultured hepatocytes (38, 39). The current data suggest that both FoxO3a and FoxO1 positively regulate expression of *SEPP1* in the basal conditions, but FoxO3a has a dominant role in the suppression of *SEPP1* downstream of metformin/AMPK pathway in H4IIEC3 hepatocytes. Interestingly, metformin selectively phosphorylated and deacetylated FoxO3a but not FoxO1 (Fig. 6, *B* and *C*). This FoxO3a-selective phosphorylation by metformin is consistent with the previous report showing that AMPK-induced phosphorylation displays a strong preference toward FoxO3 compared with FoxO1 by using *in vitro* kinase assays (16).

The current study is the first to demonstrate the decreased nuclear localization and subsequent transcriptional inactivation of FoxO3a by AMPK downstream of metformin in the cultured hepatocytes. Greer *et al.* (16) identified FoxO3a as a direct phosphorylation target of AMPK using *in vitro* kinase assays. However, the authors reported that phosphorylation by AMPK increases FoxO3a transcriptional activity without affecting FOXO3A subcellular localization in mouse embryonic fibroblasts or 293T cells. A similar activation of FoxO3a by AMPK was reported in C2C12 myotubes (17). In this respect, our results suggest that the AMPK-induced inactivation of FoxO3a is hepatocyte-specific. When FoxO proteins are phosphorylated by Akt, the dissociation of nuclear co-factors from FoxO is thought to be required for nuclear exclusion of FoxO (40). Hence, the difference in nuclear co-activator/co-repressor

recruitment between hepatocytes and other cells might explain differences in the action of AMPK on FoxO3a cellular localization and transcriptional activity. Notably, the siRNA-induced knockdown of *Foxo3a* decreased *Sepp1* and *G6pc* mRNA levels in H4IIEC3 hepatocytes, suggesting that the AMPK/FoxO3a pathway in the liver regulates gluconeogenesis and the production of the hepatokine SeP. These findings shed light on a previously unrecognized role for the AMPK/FoxO3a pathway in the regulation of glucose metabolism in the liver.

The cancellation of the metformin-induced suppression of SeP by compound C, a known inhibitor of the AMPK pathway, was only partial (Fig. 2*B*). Likewise, the overexpression of FoxO3a only partially cancelled the suppressive action of metformin on *Sepp1* gene expression (Fig. 6, *D* and *E*). These results suggest that metformin decreases *Sepp1* gene expression through both AMPK/FoxO3a-dependent and other independent pathways. Recently, Kalender *et al.* (41) reported that metformin acts to suppress mTORC1 signaling in an AMPK-independent manner. In addition, Guigas *et al.* (42) found that metformin inhibits glucose phosphorylation in primary cultured hepatocytes independently of AMPK activity. Additional studies are needed to elucidate the AMPK-independent actions of metformin on *Sepp1* expression in H4IIEC3 hepatocytes.

The present sequence of *SEPP1* promoter completely corresponds to the refseq of the National Center for Biotechnology Information, but it misses one thymidine against the sequence of a previous report (21). This site had been reported as an SNP site (reference SNP ID rs201851607). Because both allele origin and minor allele frequency of this SNP site are not available, it is difficult to prove which genome sequence is "correct." At least this SNP site does not seem to affect basal *SEPP1* promoter activity. In addition, the metformin-responsible element identified in the current paper locates in the other region of the SNP site. Thus, we consider that the effect of this SNP on the conclusion of this paper is negligible.

A limitation of the present study is that the effects of metformin on SeP expression were not investigated in human samples. The metformin concentrations used in this study (0.25–1 mM) were higher than the blood levels of metformin in patients treated with conventional doses of the drug (10–40 μM). However, it has been pointed out that concentrations of metformin in liver tissue are much higher than those in the blood because the liver receives portal vein blood, which may contain materially higher doses of metformin than plasma (43). An early report indicated that metformin concentrations in the liver were greater than 250 μmol/kg in an STZ diabetic mouse model treated with 50 mg/kg metformin (44). One previous study used 0.25–1 mM metformin in rat primary hepatocytes as a more physiological range of intrahepatic concentration (43). In addition, we show that administration of 300 mg/kg metformin was effective on hepatic expression for *Sepp1* in C57BL/6J mice (Fig. 1*F*). Although clinical trials are necessary, we speculate here that treatment with metformin decreases blood levels of SeP in patients with diabetes. Additionally, the contribution of SeP suppression to the anti-diabetic actions of metformin should be confirmed by additional investigations using *Sepp1*-knock-out mice.

In summary, the present data provide a novel mechanism of action for metformin involving improvement of systemic insulin sensitivity via the regulation of SeP production (Fig. 6*E*) and suggest that AMPK/FoxO3a pathway in the liver may be a therapeutic target to the development of new anti-diabetic drugs.

Acknowledgments—We thank Dr. Atsushi Hirao (Kanazawa University) for providing a vector for FHRE-Luc and Maki Wakabayashi (Kanazawa University) for technical assistance. We thank Fabienne Foufelle (Université Pierre et Marie Curie) for providing adenovirus vector encoding DN-AMPK. We thank In-kyu Lee (Kyungpook National University) for providing adenovirus vector encoding CA-AMPK.

REFERENCES

1. Burk, R. F., and Hill, K. E. (2005) Selenoprotein P. An extracellular protein with unique physical characteristics and a role in selenium homeostasis. *Annu. Rev. Nutr.* **25,** 215–235
2. Carlson, B. A., Novoselov, S. V., Kumaraswamy, E., Lee, B. J., Anver, M. R., Gladyshev, V. N., and Hatfield, D. L. (2004) Specific excision of the selenocysteine tRNA[Ser]Sec (Trsp) gene in mouse liver demonstrates an essential role of selenoproteins in liver function. *J. Biol. Chem.* **279,** 8011–8017
3. Schomburg, L., Schweizer, U., Holtmann, B., Flohé, L., Sendtner, M., and Köhrle, J. (2003) Gene disruption discloses role of selenoprotein P in selenium delivery to target tissues. *Biochem. J.* **370,** 397–402
4. Hill, K. E., Zhou, J., McMahan, W. J., Motley, A. K., Atkins, J. F., Gesteland, R. F., and Burk, R. F. (2003) Deletion of selenoprotein P alters distribution of selenium in the mouse. *J. Biol. Chem.* **278,** 13640–13646
5. Misu, H., Takamura, T., Takayama, H., Hayashi, H., Matsuzawa-Nagata, N., Kurita, S., Ishikura, K., Ando, H., Takeshita, Y., Ota, T., Sakurai, M., Yamashita, T., Mizukoshi, E., Yamashita, T., Honda, M., Miyamoto, K., Kubota, T., Kubota, N., Kadowaki, T., Kim, H.-J., Lee, I., Minokoshi, Y., Saito, Y., Takahashi, K., Yamada, Y., Takakura, N., and Kaneko, S. (2010) A liver-derived secretory protein, selenoprotein P, causes insulin resistance. *Cell Metab.* **12,** 483–495
6. Wang, D.-S., Jonker, J. W., Kato, Y., Kusuhara, H., Schinkel, A. H., and Sugiyama, Y. (2002) Involvement of organic cation transporter 1 in hepatic and intestinal distribution of metformin. *J. Pharmacol. Exp. Ther.* **302,** 510–515
7. Shu, Y., Sheardown, S. A., Brown, C., Owen, R. P., Zhang, S., Castro, R. A., Ianculescu, A. G., Yue, L., Lo, J. C., Burchard, E. G., Brett, C. M., and Giacomini, K. M. (2007) Effect of genetic variation in the organic cation transporter 1 (OCT1) on metformin action. *J. Clin. Invest.* **117,** 1422–1431
8. Boyle, J. G., Salt, I. P., and McKay, G. A. (2010) Metformin action on AMP-activated protein kinase. A translational research approach to understanding a potential new therapeutic target. *Diabet. Med.* **27,** 1097–1106
9. Malin, S. K., Gerber, R., Chipkin, S. R., and Braun, B. (2012) Independent and combined effects of exercise training and metformin on insulin sensitivity in individuals with prediabetes. *Diabetes Care* **35,** 131–136
10. Singh, S., Akhtar, N., and Ahmad, J. (2012) Plasma adiponectin levels in women with polycystic ovary syndrome. Impact of Metformin treatment in a case-control study. *Diabetes Metab. Syndr.* **6,** 207–211
11. Shargorodsky, M., Omelchenko, E., Matas, Z., Boaz, M., and Gavish, D. (2012) Relation between augmentation index and adiponectin during one-year metformin treatment for nonalcoholic steatohepatosis. Effects beyond glucose lowering? *Cardiovasc. Diabetol.* **11,** 61
12. Medema, R. H., Kops, G. J., Bos, J. L., and Burgering, B. M. (2000) AFX-like Forkhead transcription factors mediate cell-cycle regulation by Ras and PKB through p27kip1. *Nature* **404,** 782–787
13. Luo, X., Puig, O., Hyun, J., Bohmann, D., and Jasper, H. (2007) Foxo and Fos regulate the decision between cell death and survival in response to UV irradiation. *EMBO J.* **26,** 380–390
14. Kops, G. J., Dansen, T. B., Polderman, P. E., Saarloos, I., Wirtz, K. W., Coffer, P. J., Huang, T.-T., Bos, J. L., Medema, R. H., and Burgering, B. M.

(2002) Forkhead transcription factor FOXO3a protects quiescent cells from oxidative stress. *Nature* **419,** 316–321
15. Olmos, Y., Valle, I., Borniquel, S., Tierrez, A., Soria, E., Lamas, S., and Monsalve, M. (2009) Mutual dependence of Foxo3a and PGC-1α in the induction of oxidative stress genes. *J. Biol. Chem.* **284,** 14476–14484
16. Greer, E. L., Oskoui, P. R., Banko, M. R., Maniar, J. M., Gygi, M. P., Gygi, S. P., and Brunet, A. (2007) The energy sensor AMP-activated protein kinase directly regulates the mammalian FOXO3 transcription factor. *J. Biol. Chem.* **282,** 30107–30119
17. Sanchez, A. M., Csibi, A., Raibon, A., Cornille, K., Gay, S., Bernardi, H., and Candau, R. (2012) AMPK promotes skeletal muscle autophagy through activation of forkhead FoxO3a and interaction with Ulk1. *J. Cell Biochem.* **113,** 695–710
18. Li, X.-N., Song, J., Zhang, L., LeMaire, S. A., Hou, X., Zhang, C., Coselli, J. S., Chen, L., Wang, X. L., Zhang, Y., and Shen, Y. H. (2009) Activation of the AMPK-FOXO3 pathway reduces fatty acid-induced increase in intracellular reactive oxygen species by upregulating thioredoxin. *Diabetes* **58,** 2246–2257
19. Lützner, N., Kalbacher, H., Krones-Herzig, A., and Rösl, F. (2012) FOXO3 is a glucocorticoid receptor target and regulates LKB1 and its own expression based on cellular AMP levels via a positive autoregulatory loop. *PLoS One* **7,** e42166
20. Honda, M., Takehana, K., Sakai, A., Tagata, Y., Shirasaki, T., Nishitani, S., Muramatsu, T., Yamashita, T., Nakamoto, Y., Mizukoshi, E., Sakai, Y., Yamashita, T., Nakamura, M., Shimakami, T., Yi, M., Lemon, S. M., Suzuki, T., Wakita, T., and Kaneko, S. (2011) Malnutrition impairs interferon signaling through mTOR and FoxO pathways in patients with chronic hepatitis C. *Gastroenterology* **141,** 128–140, 140.e1–140.e2
21. Dreher, I., Jakobs, T. C., and Köhrle, J. (1997) Cloning and characterization of the human selenoprotein P promoter. Response of selenoprotein P expression to cytokines in liver cells. *J. Biol. Chem.* **272,** 29364–29371
22. Takebe, G., Yarimizu, J., Saito, Y., Hayashi, T., Nakamura, H., Yodoi, J., Nagasawa, S., and Takahashi, K. (2002) A comparative study on the hydroperoxide and thiol specificity of the glutathione peroxidase family and selenoprotein P. *J. Biol. Chem.* **277,** 41254–41258
23. Nakamura, S., Takamura, T., Matsuzawa-Nagata, N., Takayama, H., Misu, H., Noda, H., Nabemoto, S., Kurita, S., Ota, T., Ando, H., Miyamoto, K., and Kaneko, S. (2009) Palmitate induces insulin resistance in H4IIEC3 hepatocytes through reactive oxygen species produced by mitochondria. *J. Biol. Chem.* **284,** 14809–14818
24. Flicek, P., Amode, M. R., Barrell, D., Beal, K., Brent, S., Carvalho-Silva, D., Clapham, P., Coates, G., Fairley, S., Fitzgerald, S., Gil, L., Gordon, L., Hendrix, M., Hourlier, T., Johnson, N., Kähäri, A. K., Keefe, D., Keenan, S., Kinsella, R., Komorowska, M., Koscielny, G., Kulesha, E., Larsson, P., Longden, I., McLaren, W., Muffato, M., Overduin, B., Pignatelli, M., Pritchard, B., Riat, H. S., Ritchie, G. R., Ruffier, M., Schuster, M., Sobral, D., Tang, Y. A., Taylor, K., Trevanion, S., Vandrovcova, J., White, S., Wilson, M., Wilder, S. P., Aken, B. L., Birney, E., Cunningham, F., Dunham, I., Durbin, R., Fernández-Suarez, X. M., Harrow, J., Herrero, J., Hubbard, T. J., Parker, A., Proctor, G., Spudich, G., Vogel, J., Yates, A., Zadissa, A., and Searle, S. M. (2012) Ensembl 2012. *Nucleic Acids Res.* **40,** D84–D90
25. Paten, B., Herrero, J., Beal, K., Fitzgerald, S., and Birney, E. (2008) Enredo and Pecan. Genome-wide mammalian consistency-based multiple alignment with paralogs. *Genome Res.* **18,** 1814–1828
26. Wingender, E. (2008) The TRANSFAC project as an example of framework technology that supports the analysis of genomic regulation. *Brief. Bioinform.* **9,** 326–332
27. Kel, A. E., Gössling, E., Reuter, I., Cheremushkin, E., Kel-Margoulis, O. V., and Wingender, E. (2003) MATCH. A tool for searching transcription factor binding sites in DNA sequences. *Nucleic Acids Res.* **31,** 3576–3579
28. Speckmann, B., Sies, H., and Steinbrenner, H. (2009) Attenuation of hepatic expression and secretion of selenoprotein P by metformin. *Biochem. Biophys. Res. Commun.* **387,** 158–163
29. Łukaszewicz-Hussain, A., and Moniuszko-Jakoniuk, J. (2004) Liver catalase, glutathione peroxidase, and reductase activity, reduced glutathione and hydrogen peroxide levels in acute intoxication with chlorfenvinphos, an organophosphate insecticide. *Pol. J. Environ. Stud.* **13,** 303–309
30. Magwere, T., Naik, Y. S., and Hasler, J. A. (1997) Effects of chloroquine treatment on antioxidant enzymes in rat liver and kidney. *Free Radic. Biol. Med.* **22,** 321–327
31. Zhou, G., Myers, R., Li, Y., Chen, Y., Shen, X., Fenyk-Melody, J., Wu, M., Ventre, J., Doebber, T., Fujii, N., Musi, N., Hirshman, M. F., Goodyear, L. J., and Moller, D. E. (2001) Role of AMP-activated protein kinase in mechanism of metformin action. *J. Clin. Invest.* **108,** 1167–1174
32. Brunet, A., Bonni, A., Zigmond, M. J., Lin, M. Z., Juo, P., Hu, L. S., Anderson, M. J., Arden, K. C., Blenis, J., and Greenberg, M. E. (1999) Akt promotes cell survival by phosphorylating and inhibiting a Forkhead transcription factor. *Cell* **96,** 857–868
33. Eckers, A., Sauerbier, E., Anwar-Mohamed, A., Hamann, I., Esser, C., Schroeder, P., El-Kadi, A. O., and Klotz, L.-O. (2011) Detection of a functional xenobiotic response element in a widely employed FoxO-responsive reporter construct. *Arch. Biochem. Biophys.* **516,** 138–145
34. Cantó, C., Gerhart-Hines, Z., Feige, J. N., Lagouge, M., Noriega, L., Milne, J. C., Elliott, P. J., Puigserver, P., and Auwerx, J. (2009) AMPK regulates energy expenditure by modulating NAD^+ metabolism and SIRT1 activity. *Nature* **458,** 1056–1060
35. Puigserver, P., Rhee, J., Donovan, J., Walkey, C. J., Yoon, J. C., Oriente, F., Kitamura, Y., Altomonte, J., Dong, H., Accili, D., and Spiegelman, B. M. (2003) Insulin-regulated hepatic gluconeogenesis through FOXO1-PGC-1α interaction. *Nature* **423,** 550–555
36. Hosaka, T., Biggs, W. H., 3rd, Tieu, D., Boyer, A. D., Varki, N. M., Cavenee, W. K., and Arden, K. C. (2004) Disruption of forkhead transcription factor (FOXO) family members in mice reveals their functional diversification. *Proc. Natl. Acad. Sci. U.S.A.* **101,** 2975–2980
37. Haeusler, R. A., Kaestner, K. H., and Accili, D. (2010) FoxOs function synergistically to promote glucose production. *J. Biol. Chem.* **285,** 35245–35248
38. Speckmann, B., Walter, P. L., Alili, L., Reinehr, R., Sies, H., Klotz, L.-O., and Steinbrenner, H. (2008) Selenoprotein P expression is controlled through interaction of the coactivator PGC-1α with FoxO1a and hepatocyte nuclear factor 4α transcription factors. *Hepatology* **48,** 1998–2006
39. Walter, P. L., Steinbrenner, H., Barthel, A., and Klotz, L.-O. (2008) Stimulation of selenoprotein P promoter activity in hepatoma cells by FoxO1a transcription factor. *Biochem. Biophys. Res. Commun.* **365,** 316–321
40. Van Der Heide, L. P., Hoekman, M. F., and Smidt, M. P. (2004) The ins and outs of FoxO shuttling. Mechanisms of FoxO translocation and transcriptional regulation. *Biochem. J.* **380,** 297–309
41. Kalender, A., Selvaraj, A., Kim, S. Y., Gulati, P., Brûlé, S., Viollet, B., Kemp, B. E., Bardeesy, N., Dennis, P., Schlager, J. J., Marette, A., Kozma, S. C., and Thomas, G. (2010) Metformin, independent of AMPK, inhibits mTORC1 in a rag GTPase-dependent manner. *Cell Metab.* **11,** 390–401
42. Guigas, B., Bertrand, L., Taleux, N., Foretz, M., Wiernsperger, N., Vertommen, D., Andreelli, F., Viollet, B., and Hue, L. (2006) 5-Aminoimidazole-4-carboxamide-1-β-D-ribofuranoside and metformin inhibit hepatic glucose phosphorylation by an AMP-activated protein kinase-independent effect on glucokinase translocation. *Diabetes* **55,** 865–874
43. Foretz, M., Hébrard, S., Leclerc, J., Zarrinpashneh, E., Soty, M., Mithieux, G., Sakamoto, K., Andreelli, F., and Viollet, B. (2010) Metformin inhibits hepatic gluconeogenesis in mice independently of the LKB1/AMPK pathway via a decrease in hepatic energy state. *J. Clin. Invest.* **120,** 2355–2369
44. Wilcock, C., and Bailey, C. J. (1994) Accumulation of metformin by tissues of the normal and diabetic mouse. *Xenobiotica* **24,** 49–57

Research Article

EASL EUROPEAN ASSOCIATION FOR THE STUDY OF THE LIVER | JOURNAL OF HEPATOLOGY

The transcription factor SALL4 regulates stemness of EpCAM-positive hepatocellular carcinoma

Sha Sha Zeng[1], Taro Yamashita[1,2,*], Mitsumasa Kondo[1], Kouki Nio[1], Takehiro Hayashi[1], Yasumasa Hara[1], Yoshimoto Nomura[1], Mariko Yoshida[1], Tomoyuki Hayashi[1], Naoki Oishi[1], Hiroko Ikeda[3], Masao Honda[1], Shuichi Kaneko[1]

[1]*Department of Gastroenterology, Kanazawa University Hospital, Kanazawa, Ishikawa, Japan;* [2]*Department of General Medicine, Kanazawa University Hospital, Kanazawa, Ishikawa, Japan;* [3]*Department of Pathology, Kanazawa University Hospital, Kanazawa, Ishikawa, Japan*

Background & Aims: Recent evidence suggests that hepatocellular carcinoma can be classified into certain molecular subtypes with distinct prognoses based on the stem/maturational status of the tumor. We investigated the transcription program deregulated in hepatocellular carcinomas with stem cell features.

Methods: Gene and protein expression profiles were obtained from 238 (analyzed by microarray), 144 (analyzed by immunohistochemistry), and 61 (analyzed by qRT-PCR) hepatocellular carcinoma cases. Activation/suppression of an identified transcription factor was used to evaluate its role in cell lines. The relationship of the transcription factor and prognosis was statistically examined.

Results: The transcription factor SALL4, known to regulate stemness in embryonic and hematopoietic stem cells, was found to be activated in a hepatocellular carcinoma subtype with stem cell features. SALL4-positive hepatocellular carcinoma patients were associated with high values of serum alpha fetoprotein, high frequency of hepatitis B virus infection, and poor prognosis after surgery compared with SALL4-negative patients. Activation of SALL4 enhanced spheroid formation and invasion capacities, key characteristics of cancer stem cells, and up-regulated the hepatic stem cell markers *KRT19*, *EPCAM*, and *CD44* in cell lines. Knockdown of SALL4 resulted in the down-regulation of these stem cell markers, together with attenuation of the invasion capacity. The SALL4 expression status was associated with histone deacetylase activity in cell lines, and the histone deacetylase inhibitor successfully suppressed proliferation of SALL4-positive hepatocellular carcinoma cells.

Conclusions: SALL4 is a valuable biomarker and therapeutic target for the diagnosis and treatment of hepatocellular carcinoma with stem cell features.

Keywords: Cancer stem cell; Hepatocellular carcinoma; Gene expression profile; Chemosensitivity.

Received 15 March 2013; received in revised form 27 August 2013; accepted 28 August 2013; available online 6 September 2013

* Corresponding author. Address: Department of General Medicine/Gastroenterology, Kanazawa University Hospital, 13-1 Takara-Machi, Kanazawa, Ishikawa 920-8641, Japan. Tel.: +81 76 265 2042; fax: +81 76 234 4281.

E-mail address: taroy@m-kanazawa.jp (T. Yamashita).

Abbreviations: CSC, cancer stem cell; HCC, hepatocellular carcinoma; EpCAM, epithelial cell adhesion molecule; AFP, alpha fetoprotein; HpSC-HCC, hepatic stem cell-like HCC; MH-HCC, mature hepatocyte-like HCC; SALL4, Sal-like 4 (Drosophila); qRT-PCR, quantitative reverse transcription-polymerase chain reaction; HDAC, histone deacetylase; SAHA, suberoylanilide hydroxamic acid; SBHA, suberic bis-hydroxamic acid; NuRD, nucleosome remodeling and deacetylase.

Introduction

Cancer is a heterogeneous disease in terms of morphology and clinical behavior. This heterogeneity has traditionally been explained by the clonal evolution of cancer cells and the accumulation of serial stochastic genetic/epigenetic changes [1]. The alteration of the microenvironment by tumor stromal cells is also considered to contribute to the development of the heterogeneous nature of the tumor through the activation of various signaling pathways in cancer cells, including epithelial mesenchymal transition programs [2].

Recent evidence suggests that a subset of tumor cells with stem cell features, known as cancer stem cells (CSCs), are capable of self-renewal and can give rise to relatively differentiated cells, thereby forming heterogeneous tumor cell populations [3]. CSCs were also found to generate tumors more efficiently in immunodeficient mice than non-cancer stem cells in various solid tumors as well as hematological malignancies [4]. CSCs are also more metastatic and chemo/radiation-resistant than non-CSCs and are therefore considered to be a pivotal target for tumor eradication [5,6].

Hepatocellular carcinoma (HCC) is a leading cause of cancer death worldwide [7]. Recently, we proposed a novel HCC classification system based on the expression status of the hepatic stem/progenitor markers epithelial cell adhesion molecule (EpCAM) and alpha fetoprotein (AFP) [8]. EpCAM-positive ($^+$) AFP$^+$ HCC (hepatic stem cell-like HCC; HpSC-HCC) is characterized by an onset of disease at younger ages, activation of Wnt/β-catenin signaling, a high frequency of portal vein invasion and poor

prognosis after radical resection, compared with EpCAM$^-$ AFP$^-$ HCC (mature hepatocyte-like HCC; MH-HCC) [9]. *EPCAM* is a target gene of Wnt/β-catenin signaling, and EpCAM$^+$ HCC cells isolated from primary HCC and cell lines show CSC features including tumorigenicity, invasiveness, and resistance to fluorouracil [9,10]. Thus, EpCAM appears to be a potentially useful marker for the isolation of liver CSCs in HpSC-HCC. However, key transcriptional programs responsible for the maintenance of EpCAM$^+$ CSCs are still unclear.

In this study, we aimed to clarify the transcriptional programs deregulated in HpSC-HCC using a gene expression profiling approach. We found that the *SALL4* gene encoding Sal-like 4 (*Drosophila*) (SALL4), a zinc finger transcriptional activator and vertebrate orthologue of the *Drosophila* gene spalt (*sal*) [11], was up-regulated in HpSC-HCC. In adults, *SALL4* is known to be expressed in hematopoietic stem cells and their malignancies, but its role in HCC has not yet been fully elucidated [12–14]. We therefore investigated the role of SALL4 in the regulation and maintenance of EpCAM$^+$ HCC.

Materials and methods

Clinical HCC specimens

A total of 144 HCC tissues and adjacent non-cancerous liver tissues were obtained from patients who underwent hepatectomy for HCC treatment from 2002 to 2010 at Kanazawa University Hospital, Kanazawa, Japan. These samples were formalin-fixed and paraffin-embedded, and used for immunohistochemistry (IHC). A further 61 HCC samples were obtained from patients who underwent hepatectomy from 2008 to 2011; these were freshly snap-frozen in liquid nitrogen and used for RNA analysis. Of these 61 HCCs, 8 and 36 cases were defined as HpSC-HCC and MH-HCC, respectively, according to previously described criteria [8].

27 HCC cases were included in both the IHC cohort (n = 144) and quantitative reverse transcription-polymerase chain reaction (qRT-PCR) cohort (n = 61), and SALL4 gene and protein expression were compared between these cases. An additional fresh HpSC-HCC sample was obtained from a surgically resected specimen and immediately used for preparation of a single-cell suspension. All experimental and tissue acquisition procedures were approved by the Ethics Committee and the Institutional Review Board of Kanazawa University Hospital. All patients provided written informed consent.

Microarray analysis

Detailed information on microarray analysis is available in the Supplementary Materials and methods.

Cell culture and reagents

Human liver cancer cell lines HuH1, HuH7, HLE, and HLF were obtained from the Japanese Collection of Research Bioresources (JCRB), and Hep3B and SK-Hep-1 were obtained from the American Type Culture Collection (ATCC). Single-cell suspensions of primary HCC tissue were prepared as described previously [15]. Detailed information is available in the Supplementary Materials and methods. The histone deacetylase (HDAC) inhibitor suberic bis-hydroxamic acid (SBHA) and suberoylanilide hydroxamic acid (SAHA) were obtained from Cayman Chemical (Ann Arbor, MI). Plasmid constructs pCMV6-SALL4 (encoding *SALL4A*), pCMV6-SALL4-GFP, and 29mer shRNA constructs against human SALL4 (No. 7412) were obtained from OriGene Technologies, Inc. (Rockville, MD). These constructs were transfected using Lipofectamine 2000 (Life Technologies, Carlsbad, CA) according to the manufacturer's protocol.

Western blotting

Whole cell lysates were prepared using RIPA lysis buffer. Nuclear and cytoplasmic proteins were extracted using NE-PER Nuclear and Cytoplasmic Extraction Reagents (Pierce Biotechnology Inc., Rockford, IL). Mouse monoclonal antibody to human Sall4 clone 6E3 (Abnova, Walnut, CA), rabbit polyclonal antibodies to human Lamin B1 (Cell Signaling Technology Inc., Danvers, MA), and mouse monoclonal anti-β-actin antibody (Sigma-Aldrich, St. Louis, MO) were used. Immune complexes were visualized by enhanced chemiluminescence (Amersham Biosciences Corp., Piscataway, NJ) as described previously [15,16].

Quantitative reverse transcription-polymerase chain reaction (qRT-PCR)

Detailed information on qRT-PCR is available in the Supplementary Materials and methods.

IHC and immunofluorescence (IF) analyses

IHC was performed using an Envision+ kit (Dako, Carpinteria, CA) according to the manufacturer's instructions. Anti-SALL4 monoclonal antibody 6E3 (Abnova, Walnut, CA), anti-EpCAM monoclonal antibody VU-1D9 (Oncogene Research Products, San Diego, CA), and anti-CK19 monoclonal antibody RCK108 (Dako Japan, Tokyo, Japan) were used for detecting SALL4, EpCAM, and CK19, respectively. Anti-Sall4 rabbit polyclonal antibodies (ab29112) (Abnova) and vector red (Vector Laboratories Inc., Burlingame, CA) were used for double color IHC analysis. Samples with >5% positive staining in a given area were considered to be positive for a particular antibody. For IF analyses, Alexa 488 fluorescein isothiocyanate (FITC)-conjugated anti-mouse immunoglobulin G (IgG) (Life Technologies) was used as a secondary antibody.

Cell proliferation, spheroid formation, invasion, and HDAC activity assay

Detailed information on this topic is available in the Supplementary Materials and methods.

Statistical analyses

Student's *t* tests were performed with GraphPad Prism software 5.0 (GraphPad Software, San Diego, CA) to compare various test groups assayed by cell proliferation assays and qRT-PCR analysis. Spearman's correlation analysis and Kaplan-Meier survival analysis were also performed with GraphPad Prism software 5.0 (GraphPad Software).

Results

Activation of SALL4 in HpSC-HCC

To elucidate the transcriptional programs deregulated in HpSC-HCC, we performed class-comparison analyses and identified 793 genes showing significant differences in differential expression between HpSC-HCC (n = 60) and MH-HCC (n = 96) (p <0.001), as previously described [9]. Of them, 455 genes were specifically up-regulated in HpSC-HCC, and we performed transcription factor analysis using this gene set to identify their transcriptional regulators by MetaCore software. We identified four transcription factor genes, *SALL4*, *NFYA*, *TP53*, and *SP1*, that were potentially activated in HpSC-HCC (Fig. 1A). Involvement of *TP53* and *SP1* in the stemness of HCC has previously been described [17,18], but the roles of *SALL4* and *NFYA* were unclear.

We investigated the interaction networks affected by *SALL4* and *NFYA* using the MetaCore dataset. We showed that *SALL4* might be a regulator of Akt signaling (*SP1*), Wnt signaling (*TCF7L2*), and epigenetic modification (*JARID2*, *DMRT1*, *DNMT3B*) [19], and could potentially regulate two other transcriptional regulators, *SP1* and *NFYA*, through Akt and Myb signaling pathways (Fig. 1B). As a recent study indicated that *SALL4* is a direct target of the Wnt signaling pathway [20], which is dominantly activated in HpSC-HCC [9], we focused on the expression of *SALL4* in HpSC-HCC, and confirmed its up-regulation in HpSC-HCC compared

A

Transcription factors	p value	z-score
SALL4	0.0005708	3.958
NFYA	0.002483	3.267
TP53	3.923E-05	4.25
SP1	2.917E-11	6.942

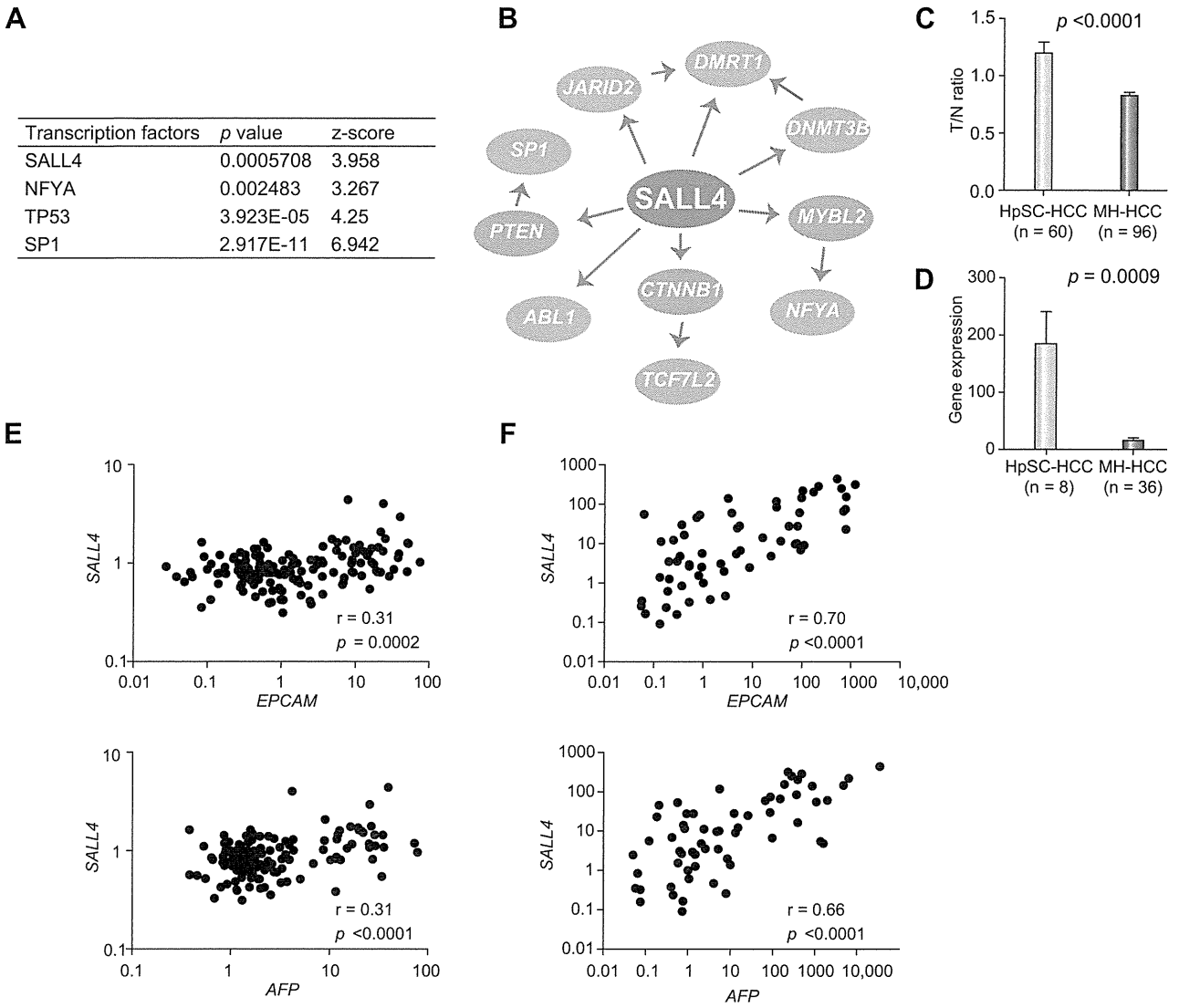

Fig. 1. Transcription factors potentially activated in HpSC-HCC. (A) Transcription factor analysis. Transcription factors regulating genes up-regulated in HpSC-HCC are listed with their *p* values and z-scores as calculated by MetaCore software. (B) Interaction network analysis. Seven genes (*ABL1*, *DMRT1*, *DNMT3B*, *JARID2*, *NFYA*, *SP1*, and *TCF7L2*, indicated in orange) shown to be up-regulated in HpSC-HCC were identified as potential target genes regulated by *SALL4* (indicated in red). (C) *SALL4* gene expression evaluated by microarray analysis. Tumor/non-tumor (T/N) ratios of microarray data in HpSC-HCC (n = 60) and MH-HCC (n = 96). (D) *SALL4* gene expression evaluated by qRT-PCR. Gene expression of *SALL4* in HpSC-HCC (n = 8) and MH-HCC (n = 36) samples. (E) Scatter plot analysis. Gene expression levels of *EPCAM* (upper panel) and *AFP* (lower panel) were positively correlated with those of *SALL4* in microarray data (n = 238, T/N ratios), as shown by Spearman's correlation coefficients. (F) Scatter plot analysis. Gene expression levels of *EPCAM* (upper panel) and *AFP* (lower panel) were positively correlated with those of *SALL4* in qRT-PCR data (n = 61), as shown by Spearman's correlation coefficients. (This figure appears in colour on the web.)

with MH-HCC as evaluated by microarray data (Fig. 1C). We validated this using an independent HCC cohort evaluated by qRT-PCR (Fig. 1D). We further examined the expression of *SALL4*, *EPCAM*, and *AFP* using microarray data of 238 HCC cases (Fig. 1E) and qRT-PCR data of 61 HCC cases (Fig. 1F). For the tumor/non-tumor ratios, we identified a weak positive correlation between *SALL4* and *EPCAM* (r = 0.31, p <0.0001) and between *SALL4* and *AFP* (r = 0.31, p = 0.0003) in the microarray cohort. We further evaluated expression of these genes in HCC tissues by qRT-PCR, and we validated the strong positive correlation between *SALL4* and *EPCAM* (r = 0.70, p <0.0001) and between *SALL4* and AFP (r = 0.66, p <0.0001) in the independent cohort.

Next we performed IHC analysis of 144 HCC cases surgically resected at Kanazawa University Hospital. We first confirmed the nuclear accumulation of SALL4 stained by an anti-human SALL4 antibody (Fig. 2A). We further confirmed the concordance of SALL4 protein expression evaluated by IHC, and *SALL4* gene expression evaluated by qRT-PCR using the same samples (Fig. 2B). We detected the nuclear expression of SALL4 in 43 of 144 HCC cases (Table 1). After evaluating the clinicopathological characteristics of SALL4-positive and -negative HCC cases, we identified that SALL4-positive HCCs were associated with a significantly high frequency of hepatitis B virus (HBV) infection and significantly high serum AFP values. We further identified that

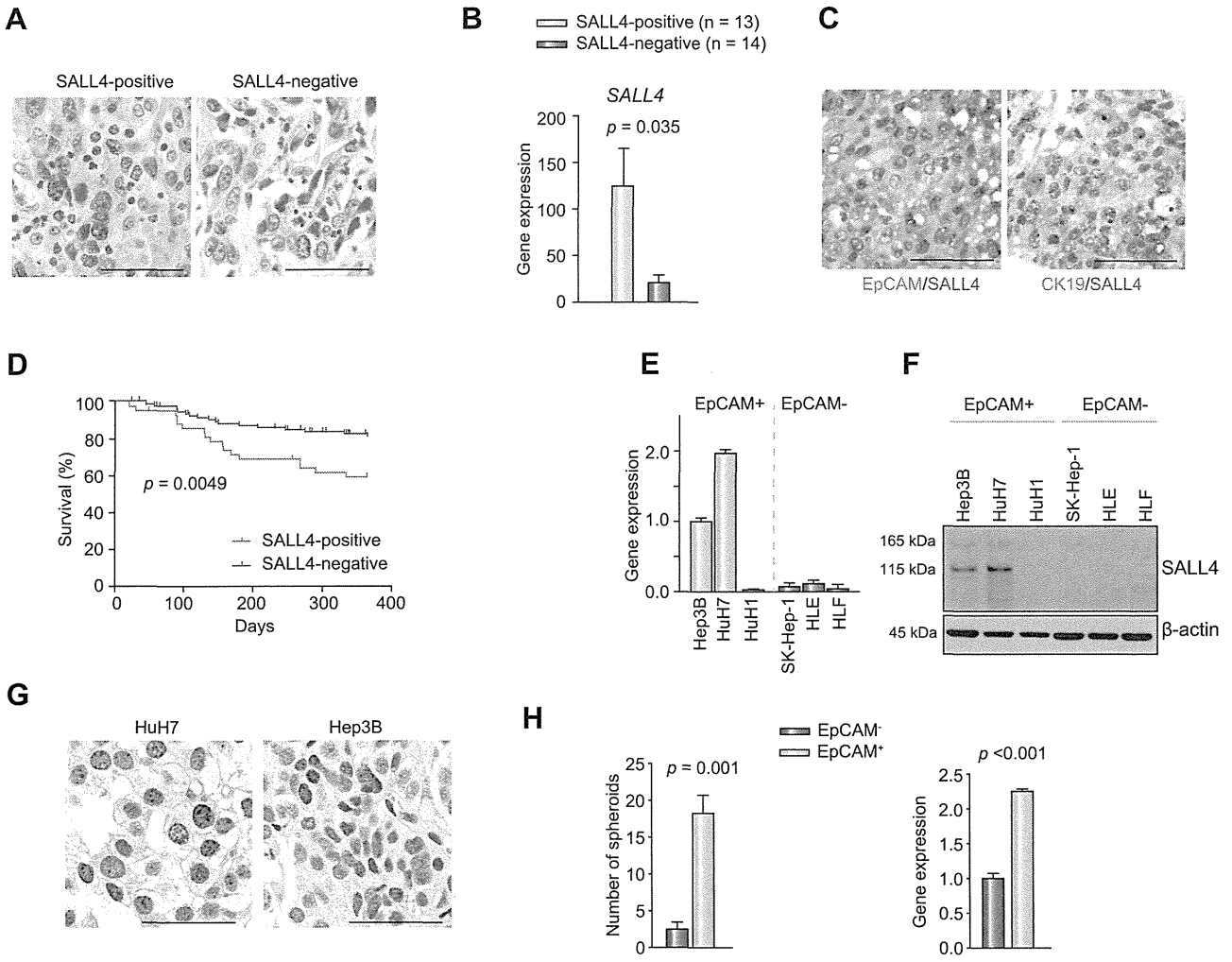

Fig. 2. SALL4 expression in human primary HCCs and cell lines. (A) Representative images of SALL4-positive and -negative HCC immunostaining (scale bar, 100 μm). (B) Gene expression of *SALL4* in SALL4-positive (n = 13) and -negative HCCs (n = 14) as shown by IHC (mean ± SD). (C) Double color IHC analysis of HCC stained with anti-SALL4 and anti-EpCAM or anti-CK19 antibodies (scale bar, 100 μm). (D) Kaplan-Meier survival analysis with Log-rank. Recurrence-free survival of SALL4-positive (n = 43) and -negative (n = 101) HCCs was analyzed. (E) *SALL4* expression in EpCAM$^+$ (Hep3B, HuH7, and HuH1) and EpCAM$^-$ (SK-Hep-1, HLE, and HLF) HCC cell lines evaluated by qRT-PCR. (F) SALL4 expression in EpCAM$^+$ and EpCAM$^-$ HCC cell lines evaluated by Western blotting. (G) IHC analysis of SALL4 expression in subcutaneous tumors obtained from EpCAM$^+$ (HuH7 and Hep3B) HCC cell lines xenografted in NOD/SCID mice. (H) Spheroid formation capacity of sorted EpCAM$^+$ and EpCAM$^-$ cells obtained from a primary HCC. Number of spheroids obtained from 2000 sorted cells is indicated (n = 3, mean ± SD). Gene expression of *SALL4* in sorted EpCAM$^+$ and EpCAM$^-$ cells obtained from a primary HCC (n = 3, mean ± SD). (This figure appears in colour on the web.)

SALL4-positive HCCs were associated with expression of the hepatic stem cell markers EpCAM and CK19. Co-expression of SALL4, EpCAM, and CK19 was confirmed by double color IHC analysis (Fig. 2C). Evaluation of the survival outcome of these surgically resected HCC cases by Kaplan-Meier survival analysis indicated that SALL4-positive HCCs were associated with significantly lower recurrence-free survival outcomes within one year compared with SALL4-negative HCCs ($p = 0.0049$) (Fig. 2D).

Because SALL4 expression was positively correlated with EpCAM and AFP expression in primary HCC cases, we evaluated the expression of SALL4 in EpCAM$^+$ AFP$^+$ and EpCAM$^-$ AFP$^-$ HCC cell lines. Consistent with the primary HCC data, two of three EpCAM$^+$ AFP$^+$ HCC cell lines (Hep3B and HuH7) abundantly expressed SALL4, as shown by qRT-PCR (Fig. 2E) and Western blotting (Fig. 2F). We identified the expression of two isoforms of SALL4 proteins with molecular weights of 165 kDa (SALL4A) and 115 kDa (SALL4B), and SALL4B was found to be the dominant endogenous isoform in HCC cell lines. All EpCAM$^-$ AFP$^-$ HCC cell lines (SK-Hep-1, HLE, and HLF) and one EpCAM$^+$ AFP$^+$ cell line (HuH1) did not express SALL4. Nuclear accumulation of SALL4 in Hep3B and HuH7 cells was confirmed by IHC using subcutaneous tumors developed in xenotransplanted NOD/SCID mice (Fig. 2G). We further evaluated the expression of *EPCAM* and *SALL4* using single cell suspensions derived from a surgically resected primary HCC. EpCAM$^+$ and EpCAM$^-$ cells were separated by magnetic beads, and we revealed a strong spheroid formation capacity of sorted EpCAM$^+$ cells compared with EpCAM$^-$ cells (Fig. 2H, left panel). Interestingly, when comparing the expression of *SALL4* in these sorted cells, we identified a high expression of *SALL4* in sorted EpCAM$^+$ cells compared with EpCAM$^-$ cells (Fig. 2H, right panel), indicating that SALL4 is activated in EpCAM$^+$ liver CSCs.

Table 1. Clinicopathological characteristics of SALL4-positive and -negative HCC cases used for IHC analyses.

Parameters	SALL4-positive (n = 43)	SALL4-negative (n = 101)	*p* value*
Age (yr, mean ± SE)	60.8 ± 1.8	64.6 ± 1.0	0.13
Sex (male/female)	27/16	70/18	0.06
Etiology (HBV/HCV/B + C/other)	21/14/0/8	20/63/3/15	0.0014
Liver cirrhosis (yes/no)	21/22	61/40	0.27
AFP (ng/ml, mean ± SE)	13,701 ± 9292	175.5 ± 55.0	<0.0001
Histological grade**			
I-II	3	18	
II-III	33	68	
III-IV	7	15	0.24
Tumor size (<3 cm/>3 cm)	17/26	57/44	0.071
EpCAM (positive/negative)	27/16	29/72	0.0002
CK19 (positive/negative)	12/31	12/89	0.027

*Mann-Whitney U-test or χ^2 test.
**Edmondson-Steiner.

SALL4 regulates stemness of HpSC-HCC

To explore the role of SALL4 in HpSC-HCC, we evaluated the effect of its overexpression in HuH1 cells which showed little expression of SALL4 irrespective of EpCAM$^+$ and AFP$^+$ HpSC-HCC phenotype. We transfected plasmid constructs encoding SALL4 (pCMV6-SALL4) or control (pCMV7), and we similarly identified the expression of two isoforms by using this construct (Fig. 3A). Evaluation of the subcellular localization of GFP-tagged SALL4 (pCMV6-SALL4-GFP) showed that it could be detected in both the cytoplasm and nucleus (Fig. 3B). We observed strong up-regulation of the hepatic stem cell marker *KRT19*, modest up-regulation of *EPCAM* and *CD44*, and down-regulation of the mature hepatocyte marker *ALB* in HuH1 cells transfected with pCMV6-SALL4 compared with the control (Fig. 3C). Up-regulation of CK19 by SALL4 overexpression was also confirmed at the protein level by IF analysis (Fig. 3D). Phenotypically, SALL4 overexpression in HuH1 cells resulted in the significant activation of spheroid formation and invasion capacities with activation of *SNAI1*, which induces epithelial-mesenchymal transition, compared with the control (Fig. 3E and F, Supplementary Fig. 1A).

We further investigated the effect of SALL4 knockdown in HuH7 cells, which intrinsically expressed high levels of SALL4. Expression of *SALL4* was decreased to 50% in HuH7 cells transfected with SALL4 sh-RNA compared with the control when evaluated by qRT-PCR (Fig. 4A). However, the reduction of SALL4 protein was more evident when evaluated by Western blotting, suggesting that this sh-RNA construct might work at the translational as well as the transcriptional level (Fig. 4B). Knock down of *SALL4* resulted in a compromised invasion capacity and spheroid formation capacity with decreased expression of *EPCAM* and *CD44* in HuH7 cells (Fig. 4C and D, Supplementary Fig. 1B and C).

SALL4 and HDAC activity in HpSC-HCC

The above data suggested that SALL4 is a good target and biomarker for the diagnosis and treatment of HpSC-HCCs. However, it is difficult to directly target SALL4 as no studies have investigated the inhibition of its transcription using chemical or other approaches [21]. We therefore re-investigated the interaction networks associated with *SALL4*, and found that SALL4 activation appeared to induce epigenetic modification (Fig. 1B). In particular, a recent study suggested that SALL4 forms a nucleosome remodeling and deacetylase (NuRD) complex with HDACs and potentially regulates HDAC activity [22]. We therefore confirmed that *SALL4* knock down resulted in the reduced activity of total HDAC in HuH7 cells (Fig. 4E). We also evaluated the effect of the overexpression of SALL4 in HuH1 and HLE cells, which do not express SALL4 endogenously, and SALL4 overexpression was found to result in a modest increase of HDAC activity and mild enhancement of chemosensitivity to an HDAC inhibitor SBHA in both cell lines (Supplementary Fig. 2A and B). We further investigated HDAC activity in two SALL4-positive (Hep3B, HuH7) and two SALL4-negative (HLE, HLF) HCC cell lines. Interestingly, high HDAC activities were detected in SALL4-positive compared with SALL4-negative HCC cell lines (Fig. 4F). The HDAC inhibitor SBHA was found to inhibit proliferation of SALL4-positive HCC cell lines at a concentration of 10 μM. By contrast, SBHA had little effect on the proliferation of SALL4-negative HCC cell lines at this concentration (Fig. 4G). SBHA treatment suppressed the expression of SALL4 gene/protein expression in SALL4-positive HuH7 and Hep3B cell lines (Supplementary Fig. 3A and B). We further investigated the effect of SAHA, an additional HDAC inhibitor, in these HCC cell lines, and SAHA was found to more efficiently suppress the cell proliferation of SALL4-positive cell lines compared with SALL4-negative cell lines (Supplementary Fig. 3C).

Taken together, our data suggest a pivotal role for the transcription factor SALL4 in regulating the stemness of HpSC-HCC. SALL4 was detected in HpSC-HCCs with poor prognosis, and inactivation of SALL4 resulted in a reduced invasion/spheroid formation capacity and decreased expression of hepatic stem cell markers. The HDAC inhibitors inhibited proliferation of SALL4-positive HCC cell lines with a reduction of SALL4 gene/protein expression, suggesting their potential in the treatment of SALL4-positive HpSC-HCC.

Discussion

Stemness traits in cancer cells are currently of great interest because they may explain the clinical outcome of patients according to the malignant nature of their tumor. Recently, we